series are compiled for eleven meteorological stations from 1961 to 2003. A longer period (from 1925) was obtained only for one station.

The location of the meteorological stations from which the data were considered sets are presented in Figure 24.

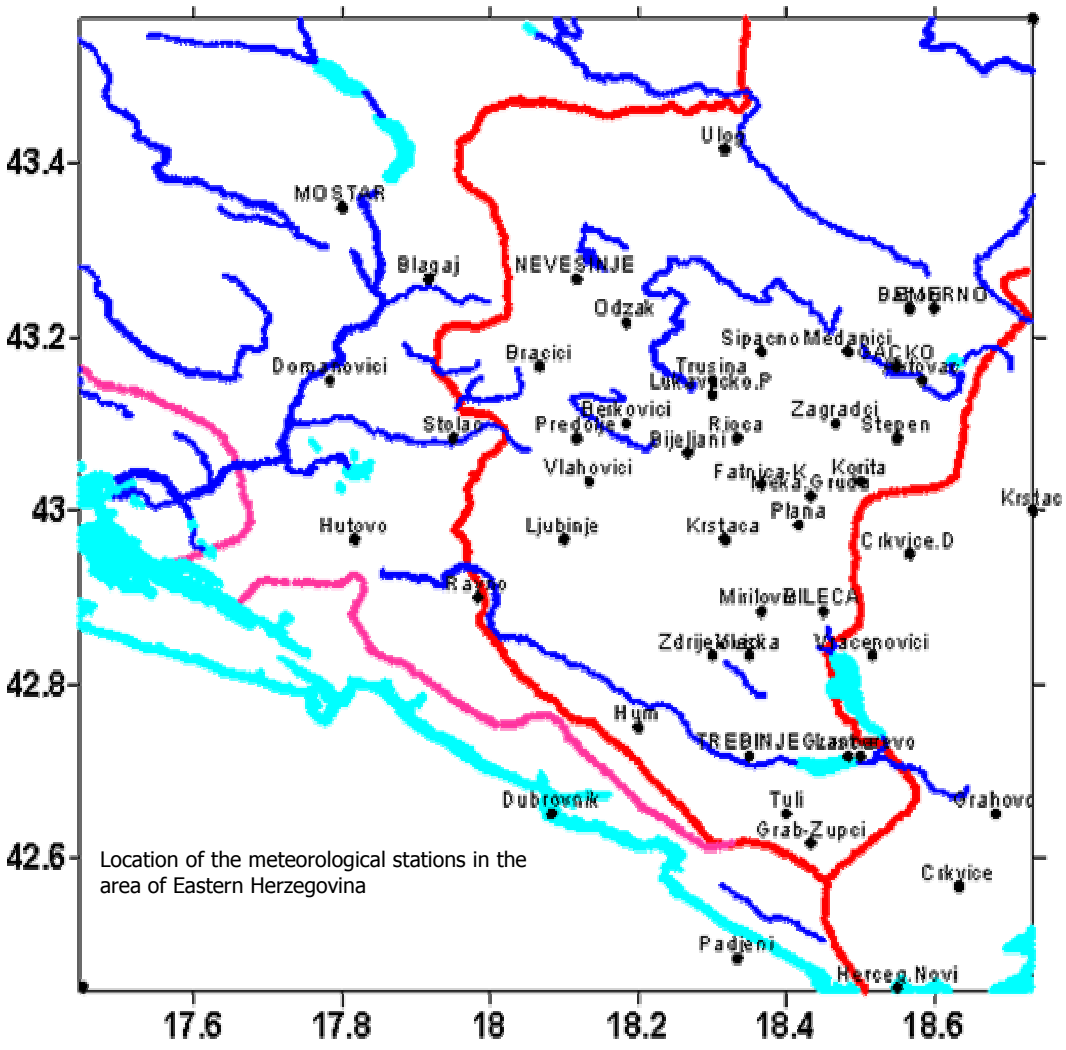

Figure 24. Location of meteorological stations in Trebišnjica catchment

For the purpose of a general climate study for the Trebišnjica catchment, all available monthly climate data for air temperature, precipitation, cloudiness, sunshine duration, wind, air humidity, as well as frequency of climate extremes for the analysed area were collected and processed (a sample shown in Figure 25). Missing values have been interpolated and spatial distribution of precipitation and air temperature was carried out on digital topography using the Gstat software.

			TREBINJE 42°43' : 18°21' 276m Karstic area/Oblast krasa								
Daily meteorological data for the period; 1January 1970-31 December 1979											
FILE FORMAT (MISSING VALUE IS 9999.0)											
Variable name, simbols and units:											
Date in yyyymmdd (year, month, day);											
u-Wind speed (24 hours) in km/d;											
Tm-Mean daily temperature on 0.1 degrees	Celsius;										
Tx-Maximum daily temperature on 0.1 degrees	Celsius;										
Tn-Minimum daily temperature on 0.1 degrees	Celsius;										
Td-Mean daily dew-point temperature in 0.1 degrees Celsius											
n-Actual sunshine hours in 0.1hrs;											
Pr-Daily precipitation amount in 0.1mm (24hours precipitation registered at 6.00UTC standard time)											
FAOP-Eto=Daily evapotranspiration in 0.1mm calculated											
according to the FAO PENMAN METHOD											
Year	**Month**	**Day**	**u**	**Tm**	**Tx**	**Tn**	**Hm**	**Td**	**n**	**Pr**	**FAOP-Eo**
#	**#**	**#**	**Km/d**	**°C**	**°C**	**°C**	**%**	**°C**	**hrs**	**mm**	**mm**
1970	1	1	355	8.9	12	6	86	6.7	0.0	47.8	0.9
1970	1	2	69	6.4	9.0	4.5	79	3.0	2.8	41.6	0.7
1970	1	3	69	3.5	6.5	0.0	81	0.6	5.5	4.0	0.5
1970	1	4	69	7.5	10.5	4.0	68	1.9	0.0	.	0.9
1970	1	5	789	12.6	13.5	6.0	81	9.4	0.0	2.2	1.5

Figure 25. A sample of daily meteorological values for Trebinje- Trebišnjica catchment area

In order to assess the consequences of potential (global) climate change on the local climate, a number of different observed gridded data sets of monthly mean values (representing large scale climatic features for the northern hemisphere) have been compiled for use as predictors in the construction of an empirical model. The data sets for the period 1960-2000, for sea level pressure (SLP), air temperature 2 m above the ground (T2m), precipitation, sea surface temperature (SST), 500hPa geo-potential heights and temperatures were compiled from information available in the web: (http://wesley.wwb.noaa.gov/cdas_data.html).

The results of experimental numerical predictions of the global climate for 100 years with a coupled atmosphere-ocean general circulation model (AOGCM) produced by Japan Meteorological Agency were applied in order to perform a local climate change assessment. From this experiment the sets of basic climate element predictions, under an assumption of a gradual increase in atmospheric CO_2 concentration at the rate of 1% per year, were extracted (the number of grid points of the global data sets is 72x46).

The spatial resolution of AOGCMs is typically a few hundred kilometres, which is probably sufficient for modelling large-scale features. However, this resolution is in general too coarse to enable these models to reproduce the climate on regional or local scale. To deduce more detailed regional and local climate scenarios it is possible to use various «downscaling» techniques of the large-scale features of AOGCMs. One approach is to apply dynamic downscaling, i.e. to use boundary conditions saved from the global predictions to «drive» a nested regional climate model. Another strategy is to use empirical downscaling. The latter is applied in this study.

3.2. Rainfall data

In order to enable hydrological model development and calibration, quality control of daily precipitation data for 51 selected meteorological stations located in the Trebišnjica catchment was performed for the period 1951-2003 (Figure 26). The period from 1951 to the 1986 was considered the best source for daily precipitation data. Daily evaporation has been computed using the FAO Penman method (Figure 25) for 5 stations for the period 1951-1979, and monthly evaporation computed for six stations for the period 1961-2030 using the Blaney-Criddle method.

TREBINJE 42°43' : 18°21' 276m Karstic area/Oblast krasa		
Daily precipitation amount in 0.1mm (P)/Dnevne količine padavina u 0.1mm (P)		
(24 hours precipitation amount registered at 6.00 UTC standard time);		
Period: 1.I 1940 - 31.XII 1986.		
FILE FORMAT (MISSING VALUE CODE IS -9999.0)		
Station name/Stanica; Date in yyyymmdd (year, month, day); P;		
TREBINJE	19400101	5.8
TREBINJE	19400102	2.8
TREBINJE	19400103	.
TREBINJE	19400104	.
TREBINJE	19400105	19.1
TREBINJE	19400106	48.5
TREBINJE	19400107	4.0
TREBINJE	19400108	.
TREBINJE	19400109	.
TREBINJE	19400110	.
TREBINJE	19400111	11.5
TREBINJE	19400112	18.2
TREBINJE	19400113	10.2
TREBINJE	19400114	

Figure 26. Daily precipitation time series for Trebinje station-Trebišnjica catchments area

Climate extremes are analysed using series of daily maximum precipitation, standardized precipitation index and days with precipitation higher than 20mm.

3.3. Identification of trends

3.3.1. Global and hemispheric temperature and precipitation trends

According to the Third Synthesis Report of the Intergovernmental Panel on Climate Change (TAR, IPCC; 2001), there is strong evidence of human influence on Earth's climate system over the last two centuries, especially in the atmosphere. The climate system has demonstrably changed on both global and regional scales since the pre-industrial era as a consequence of human influence and natural phenomena. Observations and model simulations indicate that most of the warming observed in the last 50 years is attributable to the increase in anthropogenic greenhouse gasses emissions, primarily due to the combustion of fossil fuels, agriculture, and land-use changes. Following the industrial revolution in the 1900`s the content of the greenhouse gasses in the atmosphere such as carbon dioxide, methane, nitrous oxide

and tropospheric ozone started to increase at increasing rates and was followed by an increase in the air temperature by 0.6^0C at a global level during the period 1860 to 2000. Globally, the increase in temperature occurred in two steps (Figure 27). The first in the period 1910-1945 and the second in the period 1975-2000. The increase is mainly attributed to anthropogenic activities and partly to other physical processes. On a global level, the 20th century, the last decade of the 20th century and the year 1998 have been the warmest of the last millennium (WMO, 2003).

In Western Africa, Southern Europe and the Mediterranean, climate conditions are becoming dryer.

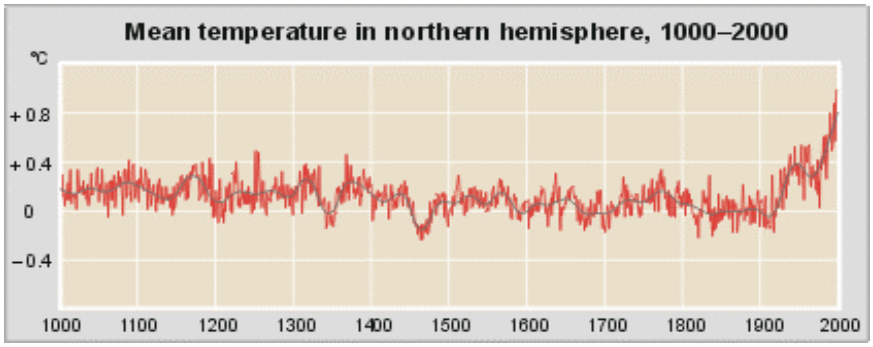

Figure 27. Mean temperature trend in northern hemisphere, 1000-2000 (From Mann et al., 1999)

3.3.2. Climate trends in Bosnia and Herzegovina and Trebišnjica catchment in the 20th century

The changes in temperature and precipitation in the area during the last century are shown in

Table 1 and

Table 2 below. During the 20th century, the climate of Bosnia and Herzegovina, and specifically the two basic parameters, precipitation and temperature show some variation which is in line to what occurred in the other parts of Southern Europe and the Mediterranean. The temperature in BiH showed an increase of 0.40^oC during the last century while precipitation has showed a reduction, but of no significant statistical importance. From the analysis of the available data the following can be concluded:

- The 1901-1940 and 1950-1970 decades were the most cold of the century for all of the areas of Bosnia and Herzegovina.
- There is a trend of temperature increase during 20th century, particular after 1970, of a rate increasing with time.

Table 1. Observed changes in the Temperature in Northern Hemisphere, Europe, the Mediterranean, Bosnia and Herzegovina and Trebišnjica catchment during the 20th century

Global-Local scales	1900-2000	Decade of 1900									
		0-10	10-20	20-30	30-40	40-50	50-60	60-70	70-80	80-90	90-00
Global scale	Increase by $0,6^0$C	+				-	-	-	+	+	+
Northern Hemisphere	Increase by $0,8^0$C	+				-	-	-	+	+	+
Europe	Increase by $0,8^0$C	+ 0.65^0C				0	0	- 0.35^0C		+	+ 0.55^0C
Eastern Mediterranean		- 0.4^0C	+ 0.70^0C		0	0	0	- 0.55^0C		+	+
Western Mediterranean	Increase by $0,8^0$C					-					+
Bosnia and Herzegovina	0.4^0C	0.0				+0.6	-0.5		+0.8		
Trebinje	0.6^0C	-0.2	0.0			+0.8	-0.9		+1.1		
Legend:	+ Increase; - Reduction; 0 Steady										

Regionally and locally, in the Trebišnjica catchment during the same period the variations were as follows:

- The meteorological stations in the Trebišnjica catchment show a trend of temperature increase in the 20th century. In this area, the temperature increased by 0.6^0C during the period 1925-2000. A significant increase in temperature occurred during the decades 1970-2000, similar to the other areas in Bosnia and Herzegovina. The year 2000 was the warmest in Bosnia and Herzegovina in the 20th century with the mean annual temperature of 2.0^0C above the normal temperature for the period 1961-1990. In Nevesinje and Trebinje the temperature seems to increase steadily since 1980 and demonstrate itself especially in warmer summers. Seasonal mean temperature for the summer months of the 1990-decade was higher by 1^0C in comparison to the mean 1961-1990 normal value, while in winter months the increase was smaller (about 0.3^0C). The summer of the 2003 was the warmest in the Trebišnjica catchment for the past 100 years.
- The precipitation in the Trebišnjica catchment is showing a reduction trend within the 20th century that is due to the reduction of the precipitation during summer, spring and winter months. During the period 1925-2000 in the

Nevesinje-Trebinje area the precipitation reduced by 6-7%, but this is not considered statistically significant.

- The decades 1950-1960 and 1980-2000 are the driest decades for the Trebišnjica catchment. During the period 1950-2003 there was a gradual reduction of precipitation, which lead to the great period of drought of the 1990s.

Table 2. Observed changes in the Precipitation in Northern Hemisphere, Europe, the Mediterranean, Bosnia and Herzegovina and Trebišnjica catchment during the 20th century.

Global-Local scales	1900-2000	Decade of 1900									
		0-10	10-20	20-30	30-40	40-50	50-60	60-70	70-80	80-90	90-00
Global scale											
Northern Hemisphere	Increase 5-10%										
North Europe	Increase 10-50%										
South Europe	Some areas Decrease										
Mediterranean	Indications reduction 5-20%						+	-	-	-	+
Bosnia and Herzegovina	Decrease 1.5%	+	+	+	+	-	+	+	-	-	+
Trebinje	Decrease 7%	-	-	-	+	-	-	+	-	-	-
Nevesinje	6%	-	-	-	+	-	-	+	-	-	-
Legend:	+ Increase; - Reduction; 0 Steady										

3.3.3. Extreme climatic phenomena

Problems related to the identification of dry and wet conditions were investigated. In particular, drought conditions in the project area were examined using the Standardized Precipitation Index (SPI). The SPI was developed by McKee et all (1993) to quantify the precipitation deficit for multiple time scales (1, 3, 6, 12, 24, 48 month). This versatility allows the SPI to monitor short-term water supplies, such as soil moisture, important for the agricultural production, and long-term water resources such as ground water supplies, streamflow and the reservoir levels. The 12 months SPI computation is based on the long-term precipitation record for the Nevesinje and Trebinje meteorological station. The SPI indicates the number of standard deviations that a particular event deviates from normal conditions. Moreover, since the SPI is normalised, wetter and drier climates can be monitored in the same way and a comparison between different locations can be made. The classification of drought and wet intensities resulting from SPI calculation is shown in Table 3.

Table 3. Standardised Precipitation Index (SPI) classification.

SPI value	**Class**

2+	Extremely wet
1.5 to 1.99	Very wet
1.0 to 1.49	Moderately wet
-0.99 to 0.99	Near Normal
-1.0 to -1.49	Moderately dry
-1.5 to -1.99	Severely dry
-2.0 and less	Extremely dry

A drought event occurs if the SPI value is -1 or less and the event ends when the index becomes positive. It mast be noted that not only the precipitation deficiency at a specific scale, but also the consecutive occurrences of deficiencies define drought severity.

Figure 28 shows that on a 12-month time scale during the last few decades the Easter Herzegovina region is affected by moderate to extreme droughts more frequently than by extreme wet conditions.

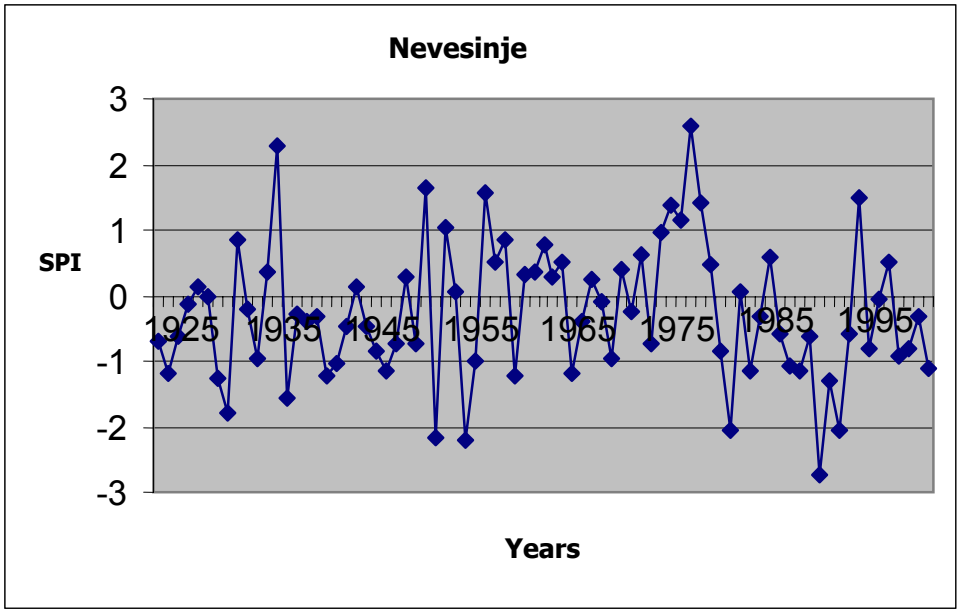

Figure 28. The monthly values of SPI on 12-month time scale for Nevesinje for the period 1925-2003

During the period 1961-2003, the frequency of days with more extreme precipitation (greater than 20mm) presents a decreasing trend for the Trebišnjica catchment (Figure 29).

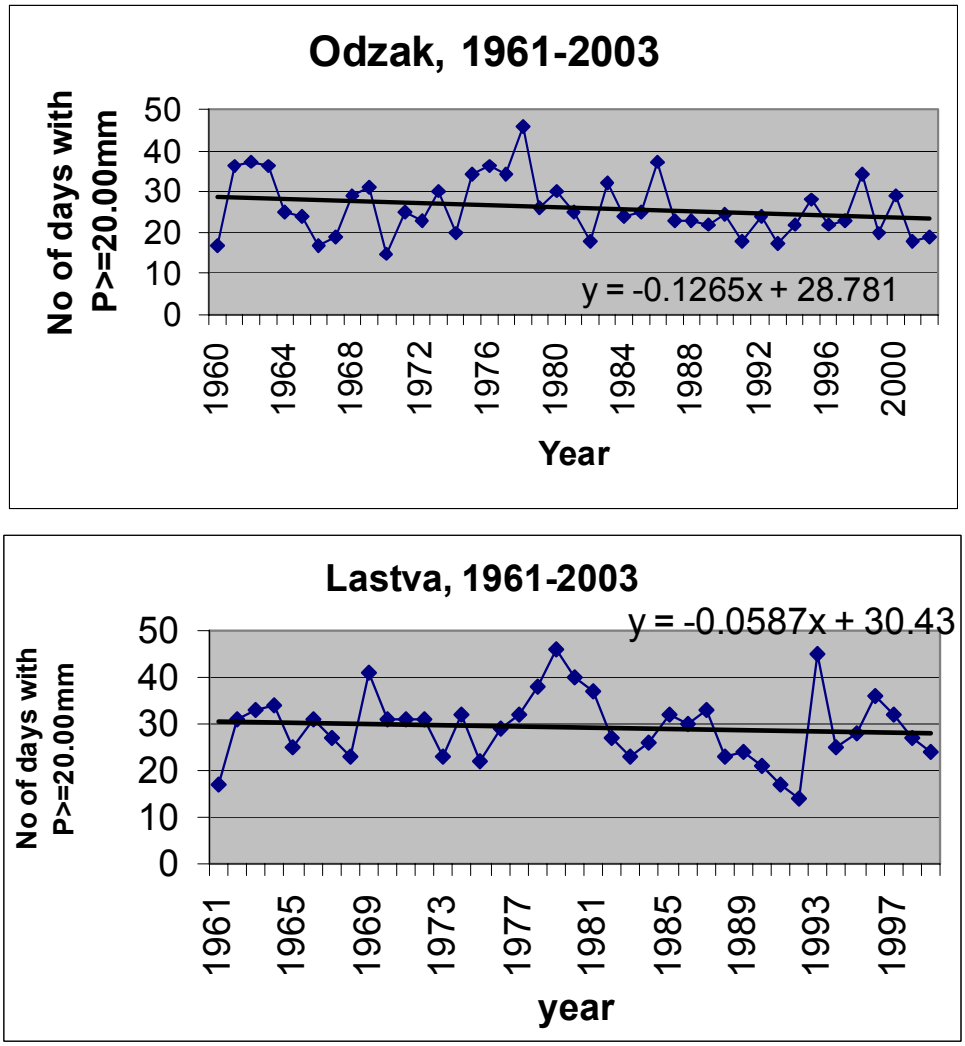

Figure 29. Extreme precipitations trend for Odžak and Lastva meteorological stations in the Trebišnjica catchment, period 1961-2003

3.4. Prediction of precipitation, evaporation and temperature under potential climate change till 2030

3.4.1. Future Climate Change

Future climate changes globally, regionally and locally shall depend on the future concentration of greenhouse gases in the atmosphere, the changes in the balance of solar radiation, and the thermal absorption of the oceans, which causes retardation to the reaction of the climate system and reduces the rate of increase of global temperature.

The size of the future climate change is estimated by the use of mathematical models that simulate all the natural processes that take place in the ocean-atmosphere-and the

sea and earth systems, which define these changes. The most frequently used models are the Atmospheric Ocean General Circulation Models (AOGCM), which evaluate the future evolution of the climatic parameters such as air temperature, precipitation, humidity and atmospheric pressure.

The latest report from the Intergovernmental Panel on Climate Change (IPCC) indicates a rise of 1.4-5.8oC in average global temperature between 1990 and 2100. This spread is the outcome of a study of twenty or so climate models and some forty scenarios of likely emissions (the scenarios included four storylines: A1F1-used to generate the High Emissions scenario; A2-used to generate the Medium-High Emissions scenario; B1-used to generate the Medium-Low Emissions scenario; B2-used to generate the Low Emissions scenario), all of which were deemed equally probable. The global climate change as consequences of these four emissions scenarios is shown in Figure 30. It is noticeable that, despite the rapid divergence of future emissions paths, the warming over the next 40 years or so is predicted to be much the same for each of the emissions paths. This is mainly due to the very long effective lifetimes of CO2 in the atmosphere and the inertia of the climate system.

According to the predictions from the climate models, precipitation is expected to increase in the Northern Hemisphere (autumn and winter) and decrease in the tropics and sub-tropics of both hemispheres. The frequency of extreme events is likely to increase with global warming.

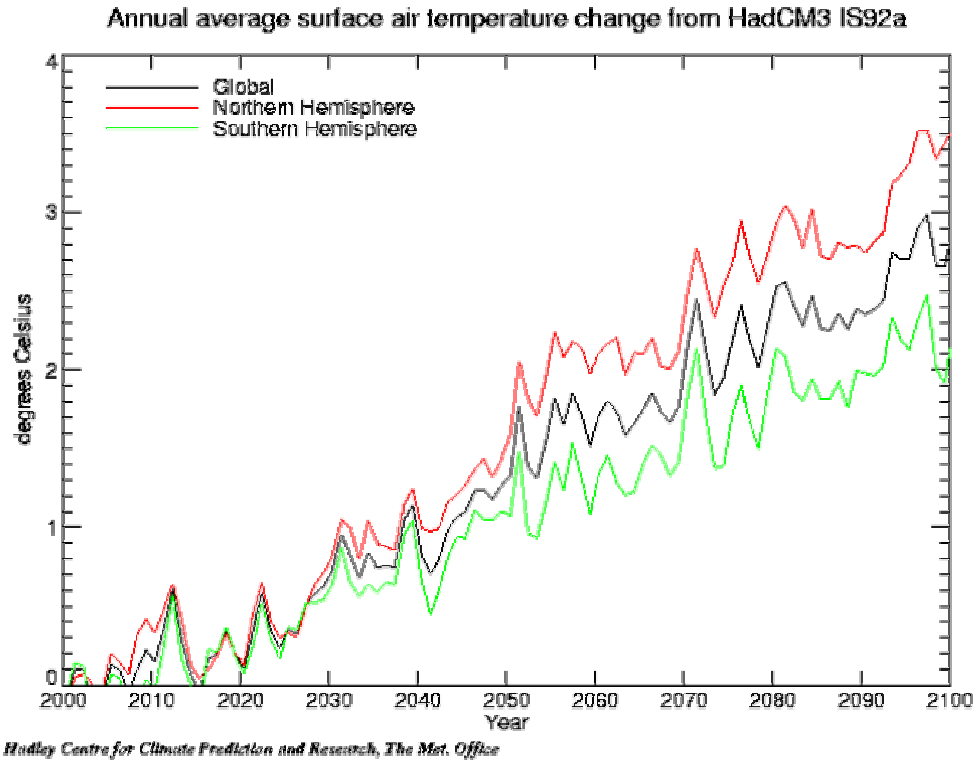

Figure 30. Projection of the annual air trend temperature for 21st century (After HADCM3 IS92a)

Climate change in Europe: From the results of different climate models it can be seen that the temperature shall rise from 0 to 4°C in the winter months depending on the latitude with higher in the Scandinavian countries, and in the summer from 0-3°C with

the greatest increase over the Southern and Central Europe. In the Southern Europe (Mediterranean region) the temperature rise in winter shall be less than that of the Northern Europe where the summer temperature rise shall be more than in North Europe. Precipitation shall increase up to 20% in Northern Europe during winter months and shall remain more or less the same during summer months. In the remaining of Europe the models usually predict a decrease in precipitation in the Mediterranean and in Central and Eastern Europe.

Mediterranean: As calculated using the global and regional climate models, the temperature is projected to increase from 0.7-1.60C per 10C of global increase (Figure 31).

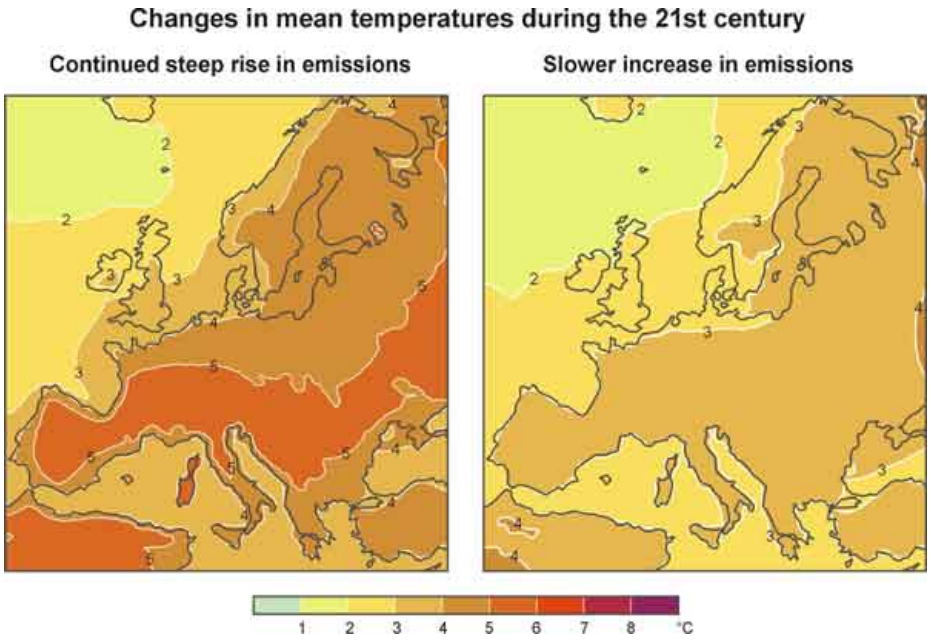

Figure 31. Changes in average annual temperature (^{o}C) 2000-2100.

The map on the left shows a continued rapid increase in emissions. The one on the right shows the result of a slower rate of increase.

During the winter period (December-February), precipitation will increase over most of the Continent. Rainfall may also be heavier. In the summer the climate will be noticeably drier, especially in southern Europe (Figure 32).

Besides a great increase in temperature, the Mediterranean region that is below the geographical latitude 450 may also suffer less rainfall. This will be especially noticeable in the summer (June-August), when the already small amounts could be halved (Figure 32).

Future climate in Bosnia and Herzegovina: By using the four climate models, Michel (2003) concluded that Bosnia and Herzegovina is expected (by 2100) to have an increase in the mean annual temperature of 1.5 to 6.7^{0}C, with an average of 3.4^{0}C, with more increase in summer temperature (average 4.6^{0}C) than in winter (average 3.0^{0}C). Precipitation is more difficult to predict since Bosnia and Herzegovina is lying in the transition zone between the Mediterranean and the Continental pluviometric regime. The studies show an decrease of the annual precipitation in Bosnia and Herzegovina up to 120mm by the 2070-2100. All the models agree that the precipitation shall decrease in summer months by 2% up to 15%.

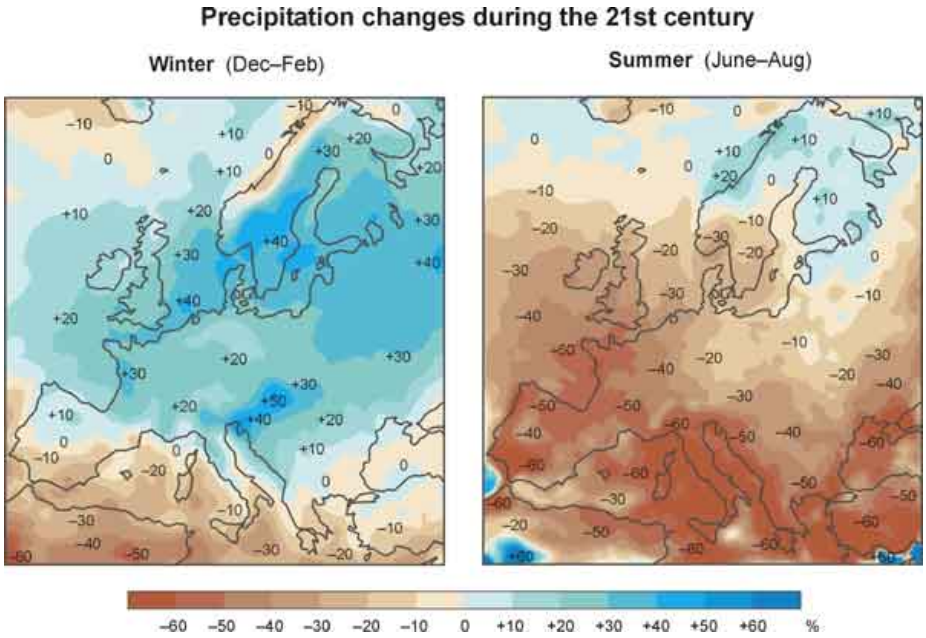

Figure 32. Changes (in per cent) in winter and summer precipitation, 2000-2100

3.4.2. Local climate scenarios for Trebišnjica Catchment based on empirical downscaling

Coupled AOGCMs are the modelling tools traditionally used for generating projections of climatic changes due to anthropogenic forcing. However, due to limited computational resources, the horizontal resolution of present day coupled AOGCMs is still of the order of a few hundred km. At this resolution, the effects of local and regional physiographic detail, like land distribution, topography and land-sea interactions on the regional climate is not fully captured. Therefore, a number of «downscaling» techniques have been developed to enhance the regional information provided by coupled AOGCMs.

One such technique is to apply dynamical downscaling, i.e. to use boundary conditions saved from the global predictions to «drive» a nested regional climate model.

The technique that was employed in this work is empirical downscaling, which is a two-step process basically consisting of:

- Development of statistical relationships between observed local climate variables (e.g. temperature and precipitation) and observed large-scale atmospheric fields (e.g. sea level pressure, surface temperature or geopotential height).
- Application of these relationships to large-scale fields simulated by GCM experiments to infer changes in local climate characteristics.

As such, empirical/statistical downscaling seeks to derive the local scale information from the larger scale through inference from the cross-scale relationships, using a random or deterministic function f such that:

local climate response = f (external, larger scale forcing)

The concept of "downscaling" does not imply that the regional climate would be determined by the large-scale state; for similar large-scale states, the associated regional states may vary substantially (Starr, 1942; Roebber and Bosart, 1998). Instead, the regional climate is seen as a random process conditioned upon a driving large-scale climate regime.

The main objectives of this study are to establish climate change scenarios (particularly for temperature and precipitation) on a local scale, with a temporal and spatial resolution appropriate for practical applications, such as water resources management. In addition, the empirical methods are well-suited for impact studies, as they can be calibrated and optimised for predefined locations and climatic parameters (Benestad, 1998b).

3.4.3. DataSets

A number of different grid data sets of monthly mean values (that represent the large scale climatic features for the northern hemisphere) have been compiled for use as predictors in the construction of empirical models. The data sets were compiled from Climate Data Assimilation System internet sites (NOAA/NCAR Reanalysis-CDAS).

The data reproduced the observed links between SLP-fields and temperatures over BiH fairly well, a fact which makes the large-scale temperature field a promising predictor for empirical downscaling of local temperatures. Hanssen-Bauer and Førland (2000b) showed that the standardized series of monthly AOGCM grid-point temperatures are related to the SLP fields in the same way as the observed series of regional standardized temperature (Hanssen-Bauer and Førland 2000a). The standardized grid-point-series may thus be interpreted as regional series, i.e. an estimate for the standardized series in a region may be found in the following way:

$$ST_m(t) \sim [T_{pm}(t) - \mu_{pm}]/s_{pm} \quad \textbf{(Equation 1)}$$

where T_{pm} is the monthly temperature series for gridpoint p in region m, while μ_{pm} and s_{pm} are mean value and standard deviation for the monthly mean temperature at this gridpoint. Local temperature series $T_{,xm}$ for any location (x) within a temperature region (m) in the Trebišnjica Catchment may then be found by the method described by Hanssen-Bauer and Nordli (1998):

$$T_{,xm}(t) \sim ST_m(t) \cdot s_{xm} + \mu_{,xm} \quad \textbf{(Equation 2)}$$

Here t is time, ST_m is the standardised monthly temperature series for region m, while μ_{xm} and s_{xm} are mean value and standard deviation for monthly mean temperature at the location x. Monthly temperature scenarios based upon the large-scale temperature field have been produced for 9 locations.

The empirical models were developed using grid-point temperature from an AOGCM integration as predictant and T(2m) from the GSM model as predictors for the period 1978-2000, using only the period 1951-1978 for model calibration. The model years 2000-2030 were used as the model evaluation period.

To account for the spatial variability of precipitation within the area, the precipitation statistics were derived for different stations in Trebišnjica catchment area. The final downscaling models, developed for different seasons, use precipitation as predictors.

The 1961-1990 climatologic and local climate projection of the analysed area shows that the area is predicted to be substantially warmer by 2030. Changes are greater in summer, ranging from 2.9 to 4.60C. Winter temperature is expected to rise by 0.5-1.2^{o} C. The annual air temperature is projected to increase from 1.9 to 2.4^{o} C, with an average of 0.5^{o} C per decade (Table 4; Figure 33; and Figure 34)

Table 4. Mean values of annual and seasonal temperature (°C) during the "normal period" 1961-90 (observations) and during the period 1991-2030 (scenarios based on empirical downscaling from the AOGSM/JMA-integration). "Diff" indicates the difference between the two periods.

	1961-90					2030				
	WIN	***SPR***	***SUM***	***AUT***	***ANN***	***WIN***	***SPR***	***SUM***	***AUT***	***ANN***
Berkovici	3.2	10.7	19.9	12.5	11.6	4.2	13.0	23.4	13.9	13.6
Bileća	3.9	11.1	20.5	12.8	12.0	4.8	13.4	24.2	14.2	14.2
Cemerno	-2.4	4.8	14.1	7.0	5.9	-1.2	7.5	17.8	8.9	8.3
Gacko	-0.4	7.3	16.8	9.1	8.2	0.6	9.7	20.3	10.6	10.3
Grancarevo	4.4	11.5	20.8	13.2	12.5	5.3	13.8	24.4	14.6	14.5
Lastva	4.4	11.4	20.9	12.9	12.3	4.9	13.8	23.8	14.2	14.2
Mostar	5.9	13.7	23.4	15.3	14.5	6.9	15.9	28.0	16.7	16.9
Nevesinje	0.3	7.7	17.1	9.3	8.6	1.2	10.1	21.1	10.7	10.8
Trebinje	6.3	13.1	22.5	15.0	14.2	7.1	15.7	26.2	16.4	16.4

	Diff [(2030)-(1961-90)]				
	WIN	***SPR***	***SUM***	***AUT***	***ANN***
Berkovici	1.0	1.3	3.5	1.4	2.0
Bileća	0.9	2.3	3.7	1.4	2.2
Cemerno	1.2	2.7	3.7	1.9	2.4
Gacko	1.0	2.4	3.5	1.5	2.1
Grancarevo	0.9	2.3	3.6	1.4	2.0
Lastva	0.5	2.4	2.9	1.3	1.9
Mostar	1.0	2.2	4.6	1.4	2.4
Nevesinje	0.9	2.4	4.0	1.4	2.2
Trebinje	0.8	2.6	3.7	1.4	2.2

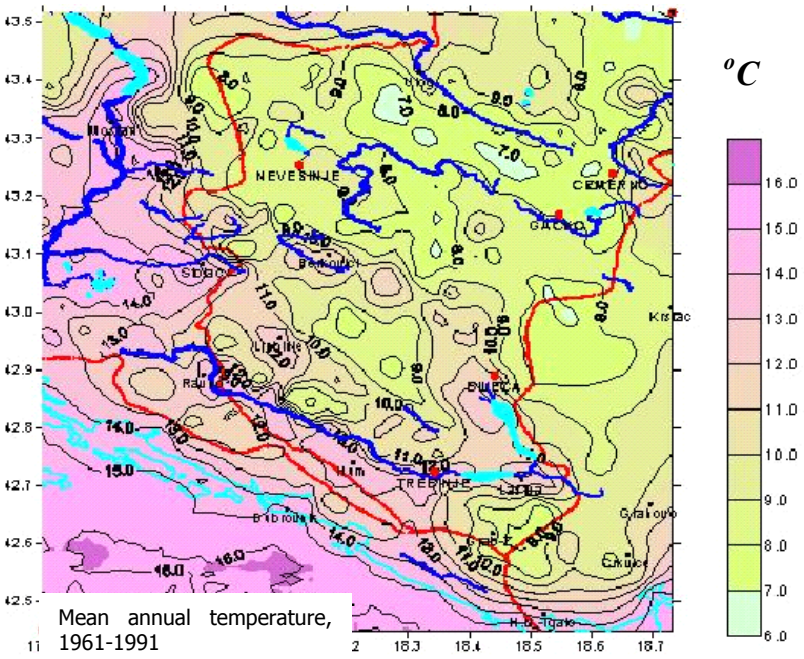

Figure 33. Spatial distribution of mean annual air temperature for the Trebinje- Trebišnjica catchment area

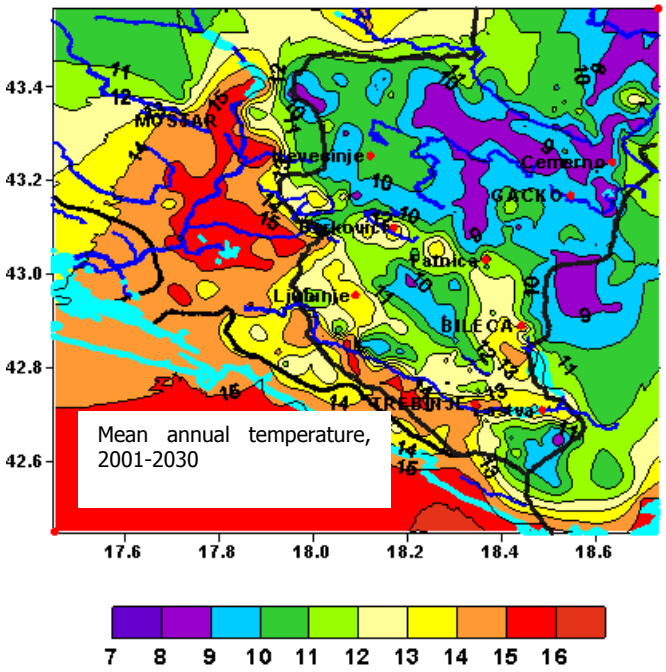

Figure 34. Spatial distribution of mean annual air temperature for Trebinje- Trebišnjica catchment area, period 2001-2030

Table 5. Mean values of annual and seasonal precipitation (0.1mm) during the "normal period" 1961-90 (observations) and during the period 1991-2030 (scenarios based on empirical downscaling from the AOGSM/JMA-integration).

	Annual and seasonal precipitation (0.1mm) 1961-1990					Precipitation changes in (%) 2030				
	WIN	SPR	SUM	AUT	ANN	WIN	SPR	SUM	AUT	ANN
Berkovici	489,7	372,9	221,7	505,9	1593,2	-38,9	-41,9	-54,5	-8,5	-36
Bileća	526,8	382,0	224,0	502,9	1633,3	-41,7	-37,8	-54,5	-6,1	-35
Čemerno	547,6	457,6	266,7	557,0	1824,5	-38,0	-39,5	-49,5	1,5	-31
Gacko	506,9	401,0	229,8	534,7	1669,6	-36,4	-39,4	-51,1	-8,7	-34
Grančarevo	500,6	321,1	193,1	532,5	1548,0	-38,4	-37,1	-52,7	-5,1	-33
Lastva	627,6	383,8	213,8	592,7	1817,2	-32,8	-31,3	-48,1	1,3	-28
Mostar	510,2	392,5	238,5	498,6	1637,0	-32,2	-37,3	-54,5	-4,8	-32
Nevesinje	567,2	445,7	242,7	535,2	1788,3	-34,8	-35,9	-54,9	-9,4	-34
Trebinje	572,7	384,9	223,7	559,3	1738,7	-35,1	-38,7	-51,9	-1,5	-32
STEPEN	496,7	382,7	228,5	471,0	1577,0	-39,9	-36,7	-50,5	-1,8	-32
TRUSINA	570,6	428,6	248,0	556,1	1807,9	-43,0	-36,7	-52,2	-4,7	-34
Average	537,9	395,7	230,0	531,4	1694.1	-37,4	-37,5	-52,2	-4,4	-33

Annual and seasonal changes in precipitation by the 2030s under the Medium-High Emissions scenario are shown in Figure 35 and Figure 36 and Table 5. In the summer, by the 2030s, rainfall is predicted to decrease by up to 50%. In the winter and spring, precipitation could decrease by 37%, whereas changes are expected to be less than 5% in autumn.

Based on the temperature projection, the evapotranspiration changes were calculated. Mean annual evapotranspiration is expected to increase by the 2030 by up to 13%.

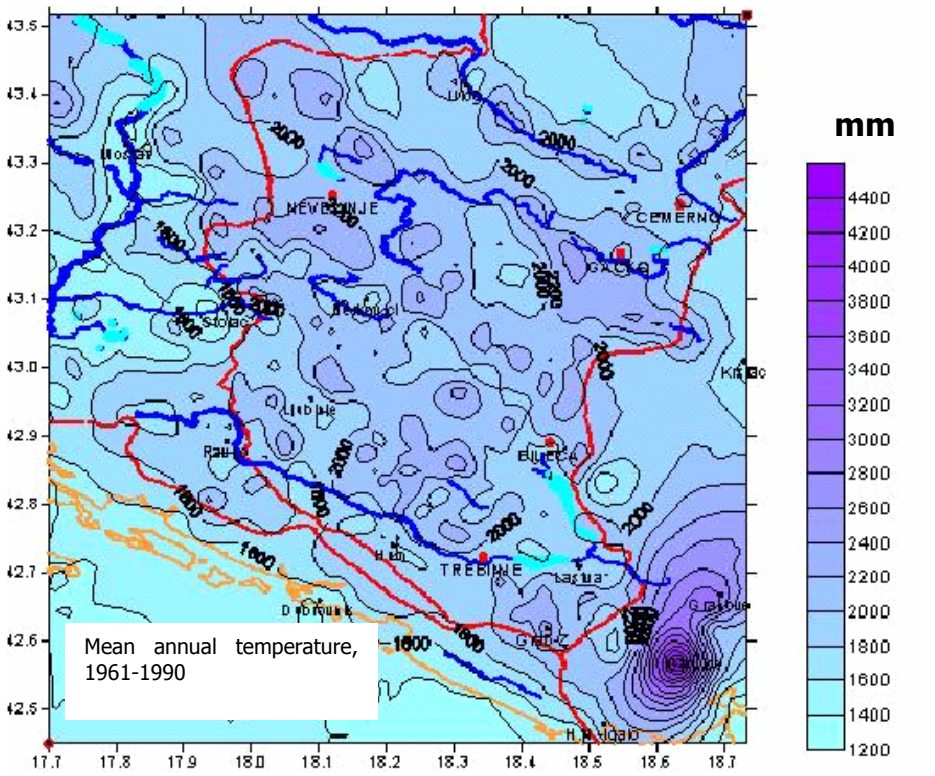

Figure 35. Spatial distribution of mean annual precipitation for Trebinje- Trebišnjica catchment area, period 1961-1990

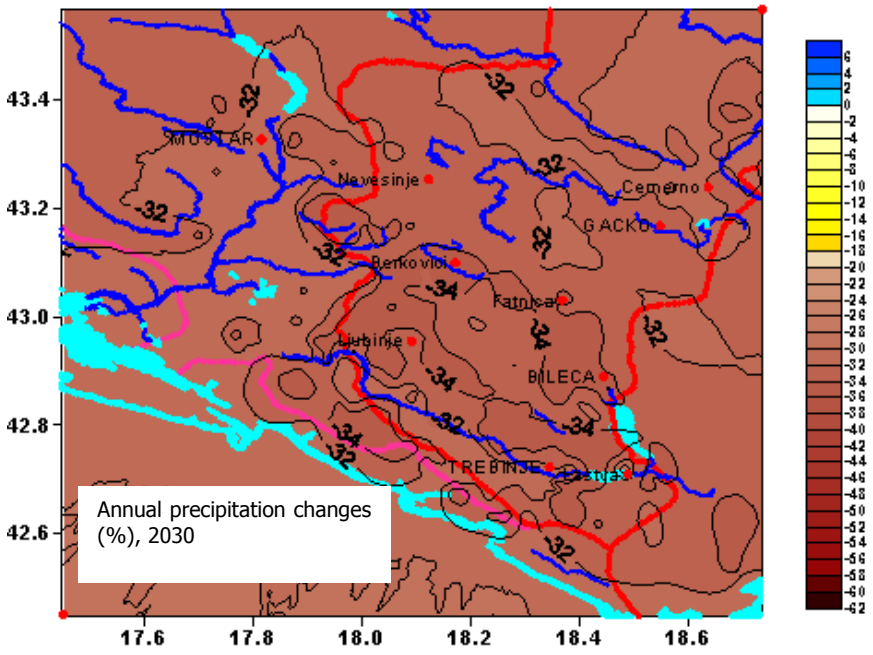

Figure 36. Annual precipitation changes up to 2030 for Trebinje- Trebišnjica catchment area

4. Topography and GIS Datasets

4.1. Data Input

The input data required to create the topography, for the wider part of both the direct and indirect catchment area of Dabarsko and Fatničko polje, was comprised of 17 digitised maps, 1:25000 scale. Maps were supplied by VGI as TIFF files, 300 DPI 256 colour images. Supplied maps were not geo-rectified.

As auxiliary data input, paper maps of scale 1:50000 were used. Paper maps were of great help during on screen digitising of finer resolution maps, as a guide for surface terrain features.

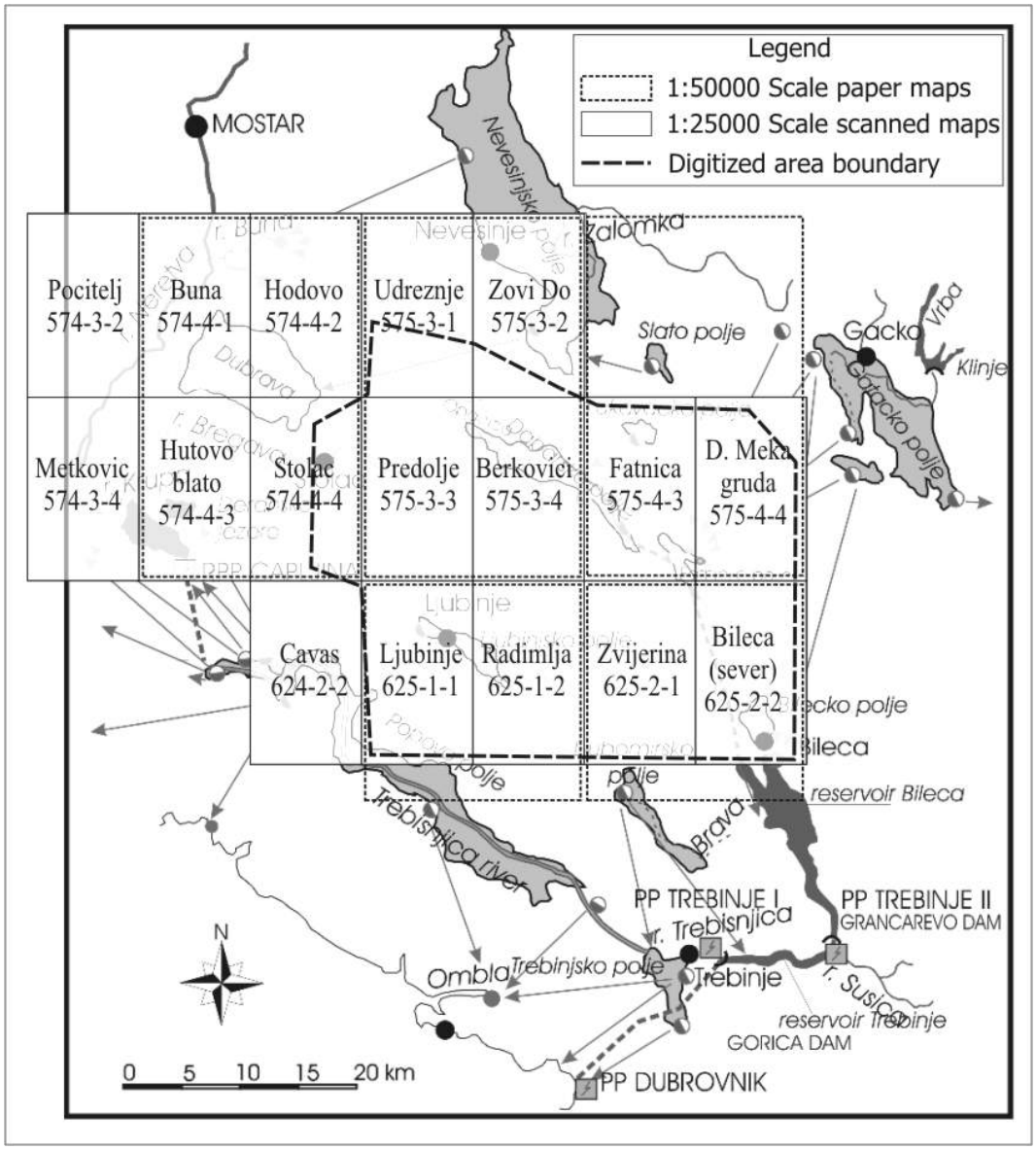

Figure 37. The broader area of Trebišnjica system with tiled maps of 1:25000 scale.

In Figure 37 the area covered by maps of scale 1:25000 is presented. As a first step, all maps were re-stretched to the proper coordinate system, and re-sampled to twice and four times lower resolutions (as 150 DPI and 75 DPI images). Multi-resolution maps were converted from TIFF format to JPG and imported into the 3DNet program using the local coordinate system. The coordinates of bottom left and top right corners of each map are shown in Figure 38.

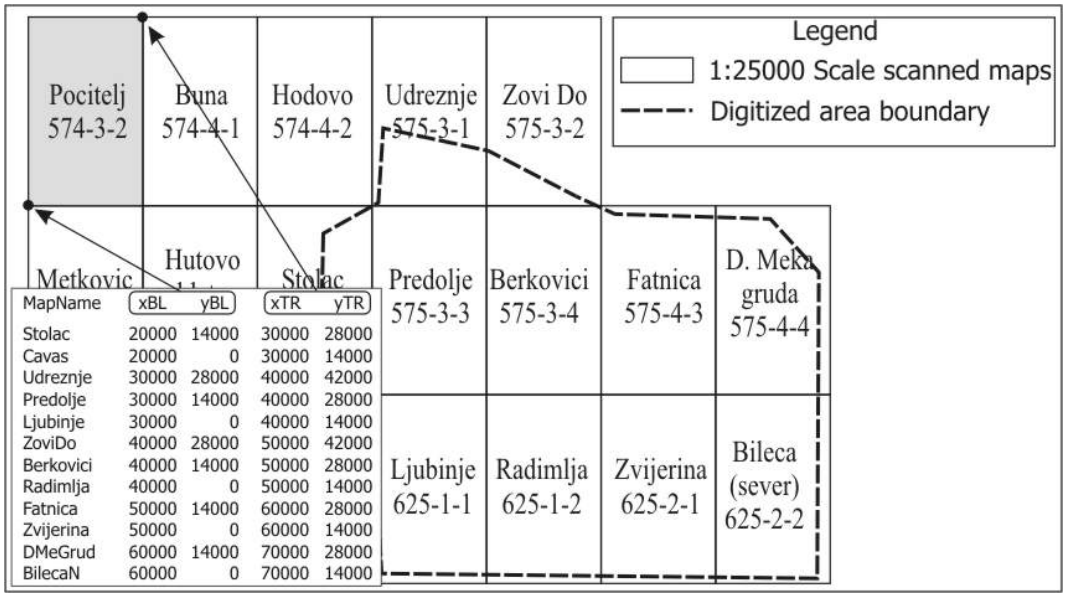

MapName	xBL	yBL	xTR	yTR
Stolac	20000	14000	30000	28000
Cavas	20000	0	30000	14000
Udreznje	30000	28000	40000	42000
Predolje	30000	14000	40000	28000
Ljubinje	30000	0	40000	14000
ZoviDo	40000	28000	50000	42000
Berkovici	40000	14000	50000	28000
Radimlja	40000	0	50000	14000
Fatnica	50000	14000	60000	28000
Zvijerina	50000	0	60000	14000
DMeGrud	60000	14000	70000	28000
BilecaN	60000	0	70000	14000

Figure 38. The coordinates of bottom left and top right corners, for each 1:25000 map

The area of interest is delineated with dashed line in Figure 37 and Figure 38. It surrounds the broader direct and indirect contributing areas of Dabarsko and Fatničko polje. The area of Gatačko polje has not been delineated in detail. Its inflows have been taken into account through Srdjeviči ponor. Since one of primary goals of the creation of a DEM was to check the stage/volume curves of Dabarsko and Fatničko polje, the biggest concern was the vertical map resolution. The supplied 1:25000 maps included 10 m contour lines, with 5 m contour lines in the lower parts of fields, and with few spot heights.

Figure 39. Comparison of two maps, with different scales but with the same content (Left: Colour coded scanned map of 1:25000 scale, Right: B&W map of 1:10000 scale but with the same content (10 m equidistance line) as the 1:25000 map

In order to have a better height resolution, a quest for a finer resolution maps was performed. Maps of 1:10000 were located, but after scanning and comparison with 1:25000, it turned out that the map content was absolutely the same, while the quality of maps was even purer. Figure 39 shows the used map (here presented in greyscale, but used in 256 colours) as well as the one that was supposed to be in 1:10000 scale.

To improve the visual representation of terrain and better feature identification, *a satellite image* of the area was also used. Figure 40 is the satellite image overlaid with the boundaries of Lukavačko, Dabarsko and Fatničko polje, while Bileća reservoir can be seen in the South-East corner.

Figure 40. Satellite image (256 colours, 15 m resolution) from GlobeXplorer, Earth Satellite Corp. with overlaid boundaries of Lukovačko, Dabarsko and Fatničko polje

4.2. Developing the DEM

The catchment area was digitised on screen within the 3DNet program. More than 73000 points and 2000 break lines were inputted, employing a thorough errors checking procedure. Figure 41 presents, for example, a common error caused by "overdigitization" of contour lines. A large number of digitised points along the contour lines (left part of figure) will, generally, produce artificial flat areas (triangles with white vertices) whereas the main terrain features, like ridges and streams are lost. Fewer points, with the inclusion of break lines (wide white line across the right part of the figure), can describe much better the terrain and preserve the main hydrological features.

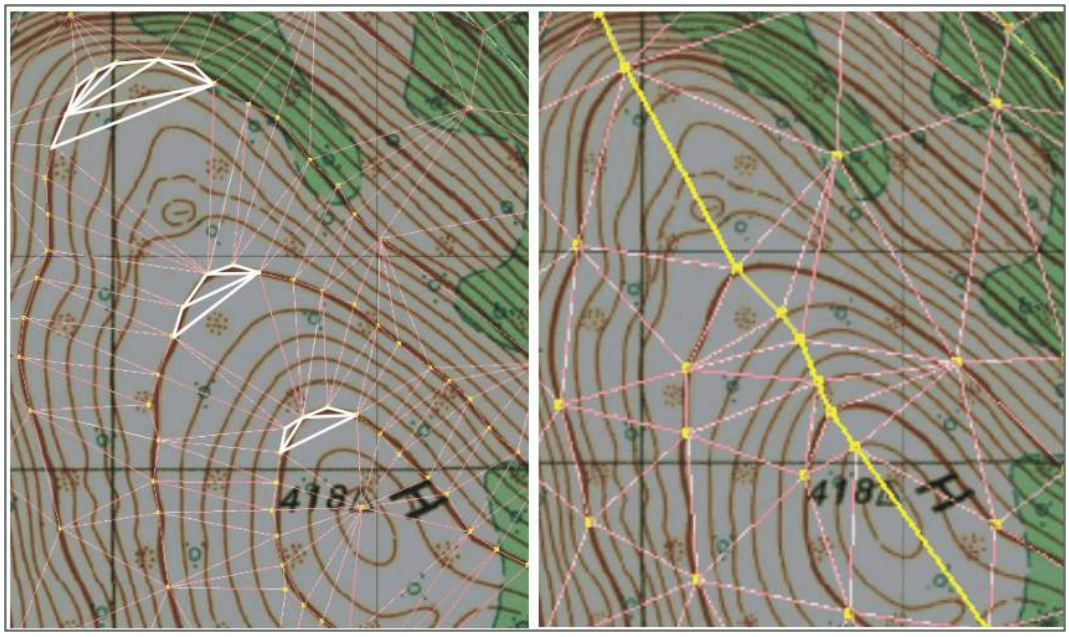

Figure 41. Large number of points digitised along the contour line does not necessarily mean better DEM: on the left figure the artificial flat areas as a result of an automatic triangulation procedure are shown with wide white line, while on the right figure, the same area is digitised with fewer points and with inclusion of break line along the ridge

Since 3DNet can overlay a number of raster images over the same area, together with scanned paper maps and satellite images, the schematic map of the Trebišnjica system, which was used by the modelling teams of the project, was re-sampled, geo-referenced, and loaded into the database. This feature improves the manageability and readability of database.

Figure 42 shows the whole catchment area digitised and triangulated. In total 30 man/days were used for the process of digitisation and data check, and 3 man/days for map correction. Special attention was paid on the flat parts of the Dabarsko polje, with Opacica stream, streams from Vrijeka and Pribitu to Ponikva, from Ljelješnica to Ponikva and small streams flowing to Kuti, and to Fatničko polje with streams coming from Baba and Obod to Pasmica.

Horizontal positional error can be assessed to be within 2 pixels on scanned map. With 300 DPI on 1:25000 map, this error is less then 5 m. Vertical resolution can be assessed to be better than 5 m within flat areas.

Once the terrain had been digitised, it was possible to "fly over" the terrain and inspect it from different angles, with draped satellite image or scanned maps. Figure 43 provides an example of such an operation, with a view along Fatničko polje towards Dabarsko polje. Using this feature, it was easy to recheck the assumed catchment boundary, and to correct it. Some smaller data errors were also detected and corrected during this visual data inspection.

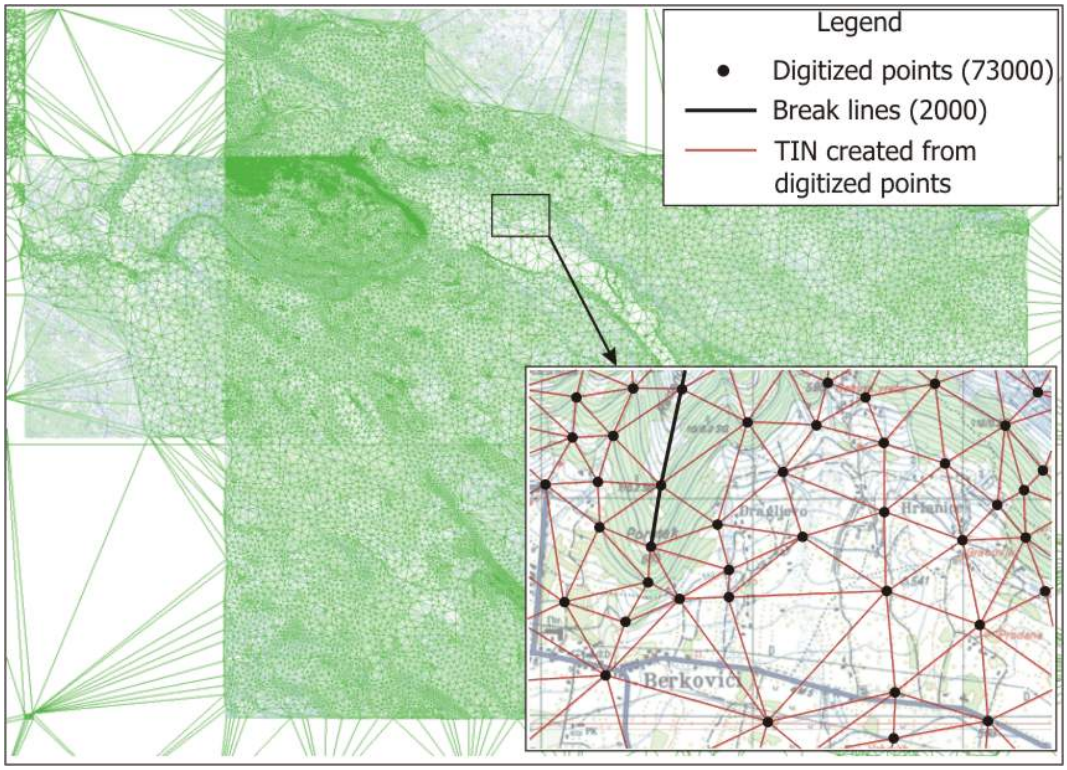

Figure 42. On screen digitised catchment area, with 73000 points and 2000 break lines

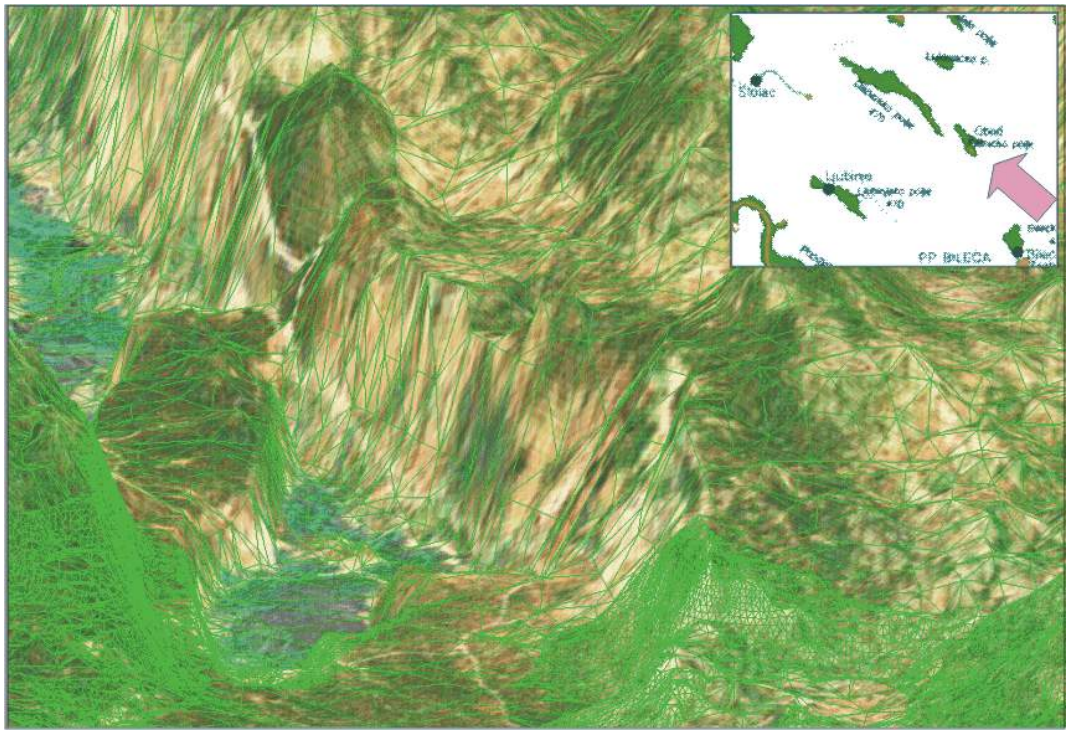

Figure 43. Side view on Fatničko polje with the SouthEast part of Dabarsko polje

From the vector TIN model, used within the 3DNet program, a regular grid DEM was created in IDRISI (raster) data format, using different grid sizes. The whole catchment area was exported with a grid size of 30 m, while two detailed DEM's of Dabarsko and Fatničko polje were created with 20 m grid size. The DEM was corrected for small errors in slope along the vertices of triangles on the break lines, using the "burn-in" procedure, so natural terrain features were preserved. Figure 44 presents the DEM of the whole catchment area.

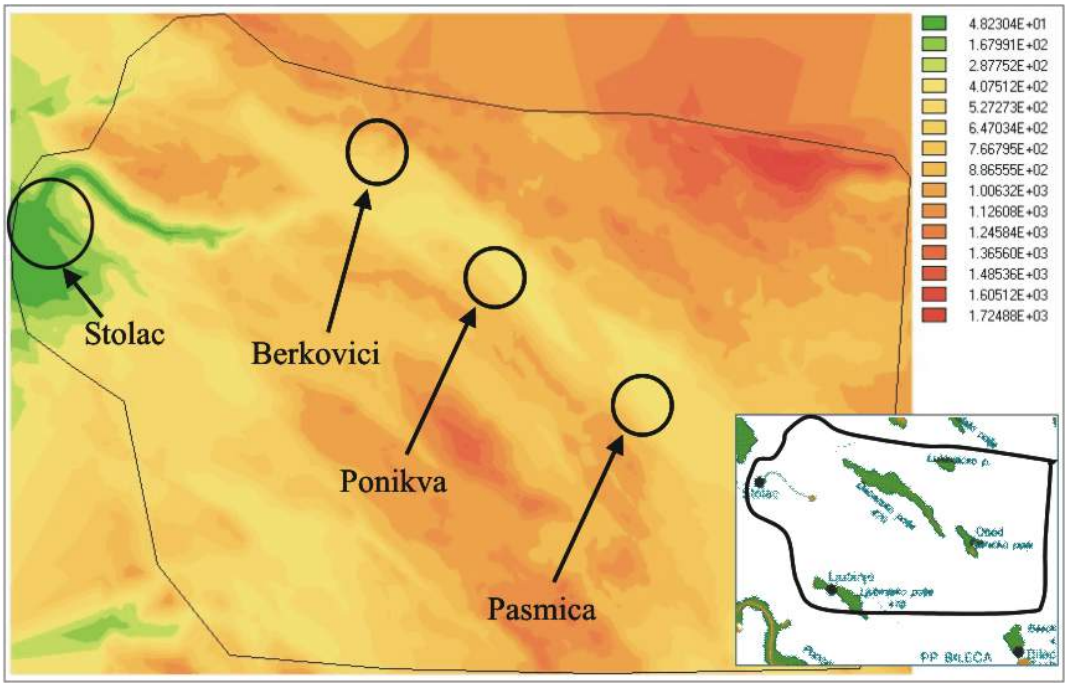

Figure 44. Regular grid DEM with 30 m resolution, heights are from 48 m to 1750 m

4.3. Catchment Delineation

Having the DEM in IDRISI GIS software, a number of spatial analysis steps were performed including calculation of slopes and directions of steepest slopes, profiles along the DEM for selected cut-line (presented in Figure 45), extraction of areas with slopes smaller then certain threshold (as check for existence of flat areas), etc.

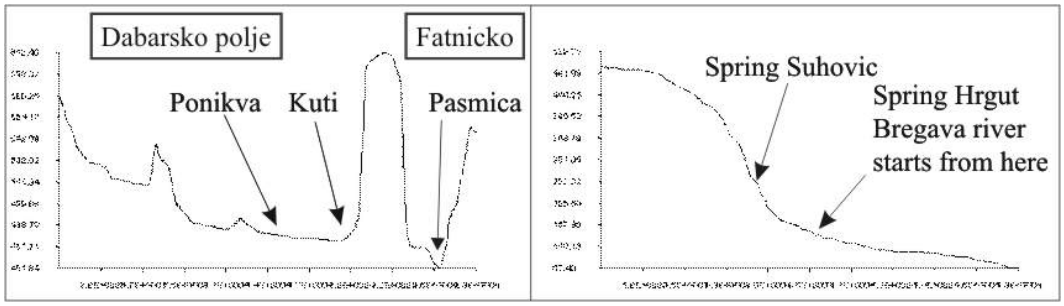

Figure 45. DEM can be used to plot the profiles along selected lines: the first image is the cut along the Dabarsko and Fatničko polje, the second one is the cut along the Bregava river

The DEM of Dabarsko polje and Fatničko polje was used, also, to delineate the natural pond boundaries, and to find the stage/area and stage/volume data. The algorithm allows detection of multiple overlaid ponds, and will detect the exit point for each pond.

Figure 46 presents the DEM of Dabarsko polje, while Figure 47 presents the Stage-Volume curve. The Stage-Area data are given in the accompanying table.

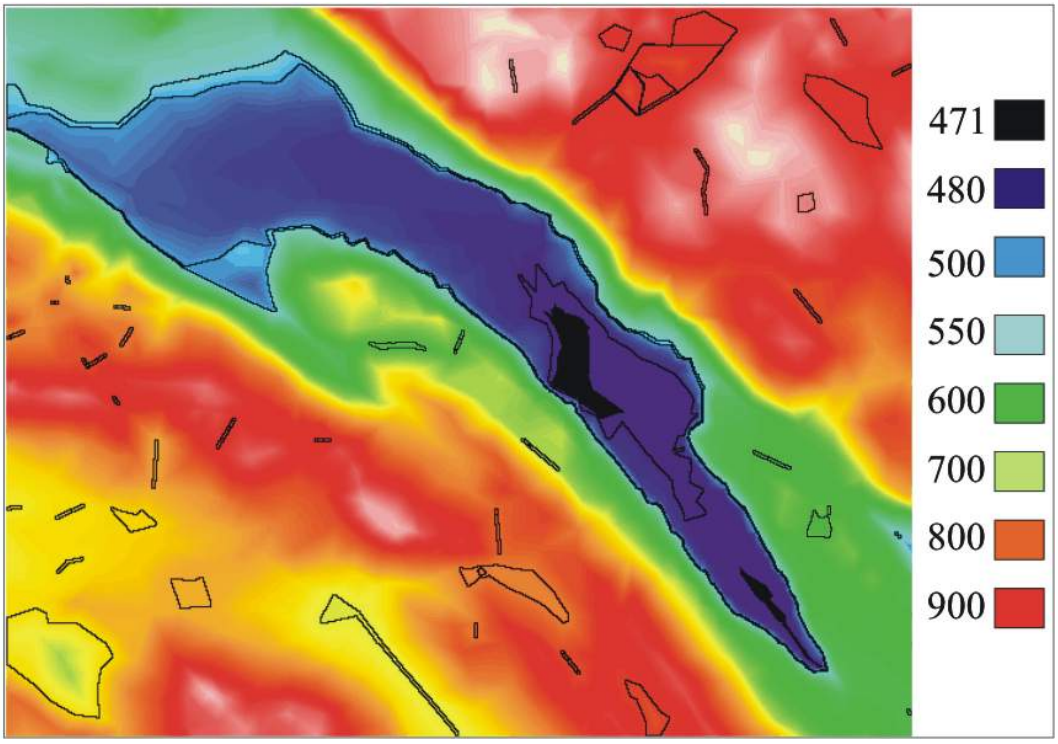

Figure 46. Digital Elevation Model (DEM) of Dabarsko polje, 20 m grid size

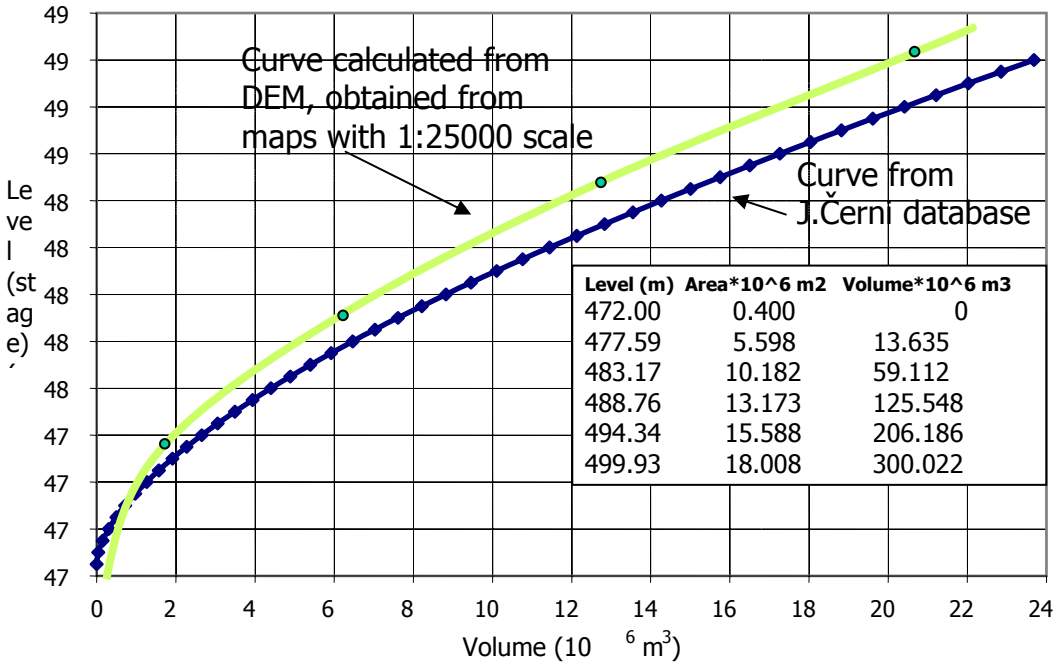

Figure 47. Stage-Volume curve and data for Stage-Area curve of Dabarsko polje

In Figure 47 the Stage-Volume curve **for Dabarsko polje** was plotted and compared with the curve obtained from Jaroslav Černi database. The curve calculated from DEM has smaller volumes for the same height, with the average reduction of 20%. Tests using a

simple physical based simulation surface-runoff model were performed using both Stage-Volume curves. The computed levels in Dabarsko polje, calculated using the original curve supplied by the Jaroslav Černi Institute, were almost impossible to calibrate with the measured water levels. On the other hand, the physical model with Stage-Volume curve produced from the DEM has shown almost ideal match with the measured data. This curve was used by the modelling teams.

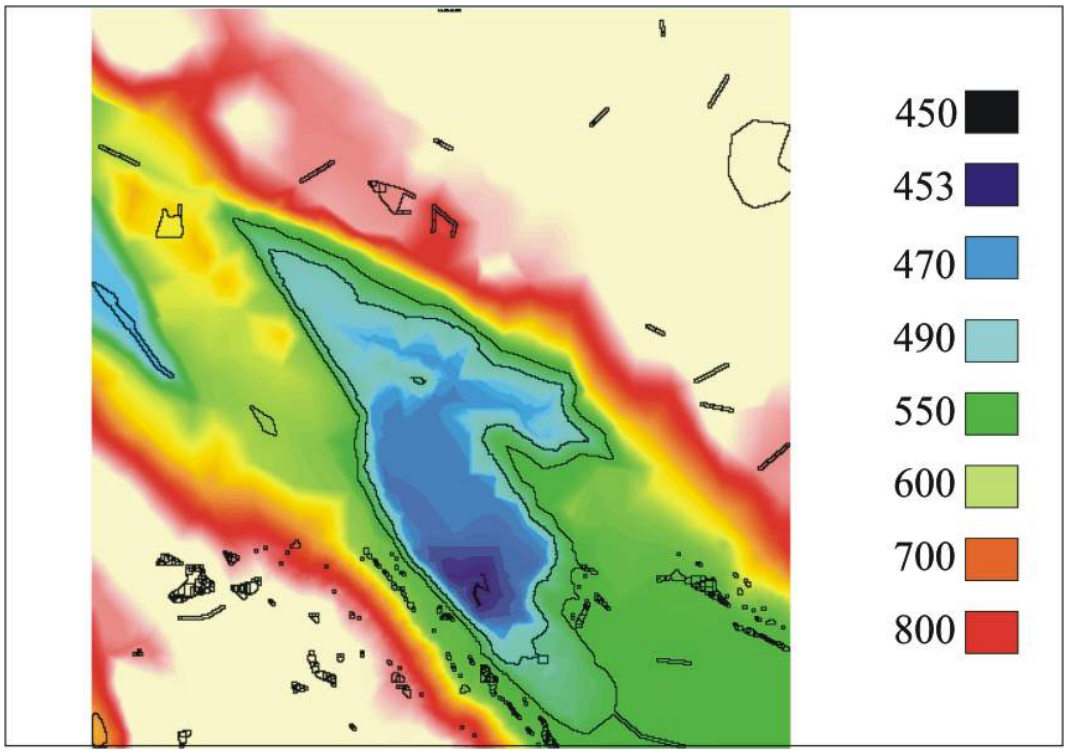

Figure 48. Digital Elevation Model (DEM) of Fatničko polje, 20 m grid size

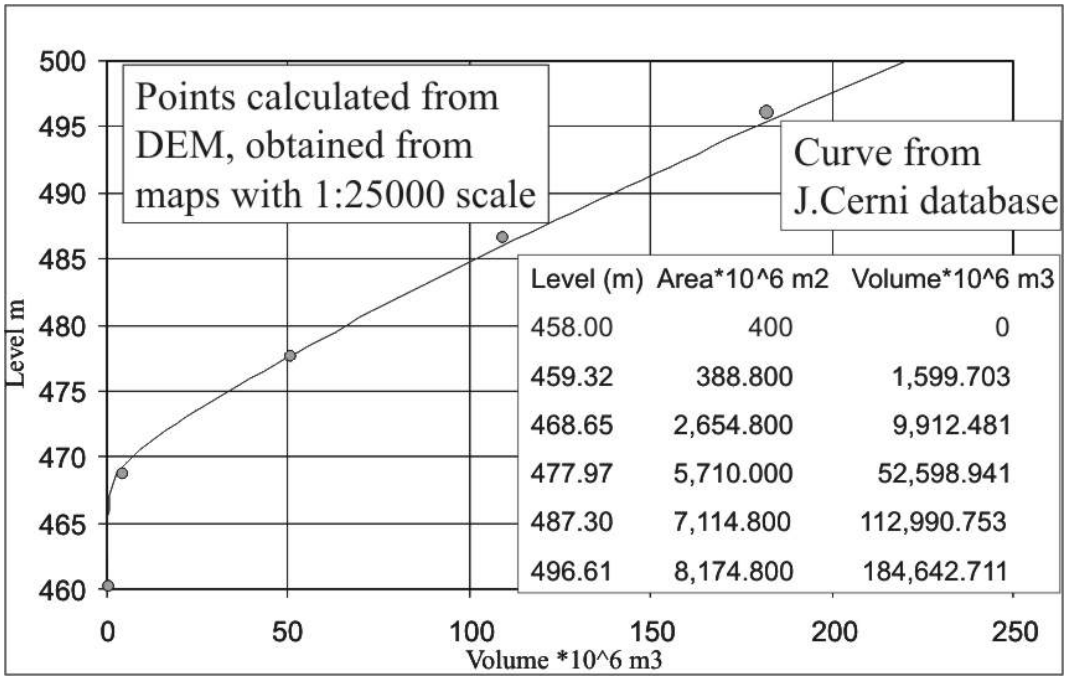

Figure 49. Stage-Volume curve and data for Stage-Area curve of Fatničko polje

Figure 48 and Figure 49 present the DEM **for Fatničko polje** and the Stage-Volume data. The original curve supplied by the Institute Jaroslav Černi (plotted as a continuous line) was almost the same as calculated one from the DEM (presented as dots).

The final result of DEM analysis are contributing areas for selected recipients: 1) Kuti, 2) BabaJama, 3) Obod, 4) Obod+Baba, 5) Bacevica (NW catchment of Fatnica), 6) Obod-Pasmica, 7) Ljeljesnica, 8) Vrijeka, 9) Pribitu, 10) Ponikva as sum of Ljeljesnica, Vrijeka and Pribitu, 11) Strupici (ponors in central south part of Dabarsko polje), 12) Lukavačko polje, 13) Opacica, 14+15) Trusinjsko polje, 16) Indirect contributing area, 17) Direct contributing area. Areas were delineated according to DEM aspects, direction of steepest slope. The boundaries of contributing areas are shown in Figure 50, together with the total areas and mean slopes.

no	Ha	AvgSlope %
1	1357.8300	22.18
2	593.9100	18.58
3	527.3100	20.29
4	86.6700	14.69
5	1629.9000	18.89
6	1999.1699	17.32
7	2247.3899	19.48
8	456.2100	25.80
9	2731.4999	19.65
10	134.3700	21.49
11	1170.2700	24.42
12	1191.5100	18.39
13	4393.4399	21.51
14	553.6800	20.83
15	360.0000	19.68
16	3130.000	
17	23700.000	

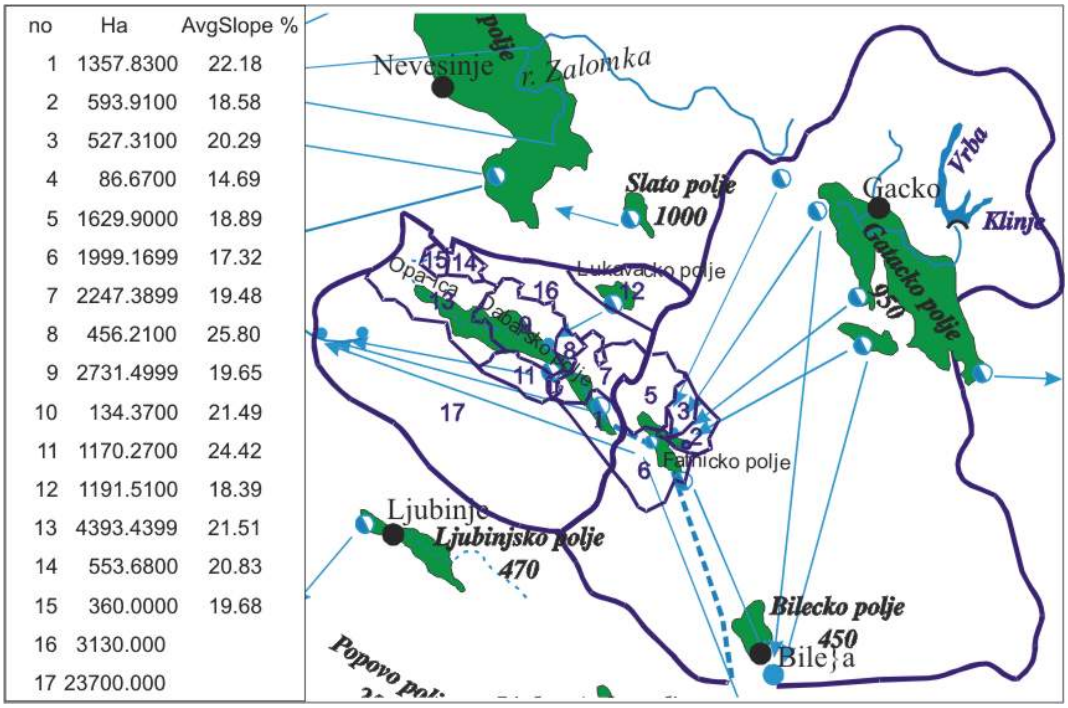

Figure 50. Contributing areas with added one indirect (16) and one direct contributing area (17), with mean terrain slope

5. Modelling

Given the importance of the problem under investigation, the research team decided to improve the reliability of the results by using *three different modelling groups* applying different modelling approaches, different levels of modelling area coverage and temporal and spatial discretisation as well as different solving algorithms. It is envisaged that each independent approach serves as a quality assurance mechanism for the rest. All three groups have been given the same datasets, the same set of operational rules, the same geometrical characteristics of the polje, the same capacity functions of the tunnels and very limited time to fine tune their models. They have all been asked to concentrate on providing an unbiased assessment of *the effect of the water transfer from Dabarsko to Fatničko polje and from Fatničko polje to Bileća reservoir using the hydrometric station Do as the reference point*. However the modelling groups have been left free to use their own scientific and professional expertise, modelling skills and to draw their own conclusions based on the results of their modelling. These results are presented and discussed in the following paragraphs. The presentation starts with the two hydrologic models (the Černi and the K Sim^2) and is concluded with a presentation of a physically-based model (3DNet).

5.1. The J. Černi Hydrologic Model

5.1.1. Model description

Introduction

The mathematical model for the definition (simulation) of the Bregava River discharge at the gauging station Do constitutes a limited part of the overall Trebišnjica river basin simulation model, which was developed as part of the Trebišnjica Hydro Information System (the Trebišnjica HIS). Under the Trebišnjica HIS, the simulation model is the core of the system comprised of the following components:

- Mathematical simulation software,
- User communication software, and
- Database.

The model was designed to allow the variation of specific parameters and the appreciation of system behaviour in different situations:

- Varying hydrologic parameters (new knowledge, modification of operating conditions, degree of system completeness, etc.),
- Different scenarios of varying user demand (hydropower, water supply, irrigation, environment, etc.), and
- Modification of system configuration.

The model was made to allow rapid and simple decision making related to ongoing system development and system management under normal and extreme conditions. In order to assure the function of the Trebišnjica HIS simulation model, it is necessary to provide for adequate generation and organization of a database to include: hydro-meteorological data, hydrogeologic data, information on the users and information on system configuration. In view of the multi-fold function of the simulation model, the database needs to include:

- The history, i.e. time series for the preceding period of observation,

- Forecast data and generated time series for the planned (future) period, and
- Real-time data, as required for short-term and mid-term system management.

In the specific case, when the impacts of certain works and measures on the Trebišnjica HIS have to be assessed, such as the transfer of water from Dabarsko Polje to Fatničko Polje and from Fatničko Polje to the Bileća reservoir, the simulation model is applied over a limited area and with selected functions (rainfall-runoff, flood routing, flow transformation through the porous medium). In such a case only the hydro-meteorological history from the generated and updated database will be used.

Decomposition of the considered area

The considered drainage area of the Bregava River to the gauging station Do covers the territory of the Cemerno mountain range, from where waters of the Vrba and Mušnica rivers and the Gatačko Polje and Černičko Polje watersheds are drained into Fatničko Polje and on to the Bileća reservoir. Water from the Dabarsko Polje watershed are drained into Fatničko Polje and the Bregava River catchment area. A part of the water from Fatničko Polje is also drained into the Bregava River catchment area, and the remainder into the Bileća reservoir.

The creation of water flow in the considered drainage area is a very complex process. This process may be studied by a systematic approach, or based on the assumption that the drainage area is a single hydrological system where the input is precipitation and the output is the exit profile flow. In the specific case the latter includes the flow at the Do station profile on the Bregava River and the Grančarevo HPP dam profile on the Trebišnjica River.

The considered area includes reservoirs, such as the Bileća reservoir on the Trebišnjica, the Vrba reservoir on the Vrba and the Klinje reservoir on the Musnica. Furthermore, karst plains: Dabarsko Polje, Fatničko Polje, Gacko Polje and Černicko Polje are significant in the transformation of flood waves in the drainage area. Between these plains the water flows through a porous karst medium.

Taking into account the stated areal and functional complexity of the system, the area was decomposed and various components were introduced which simulate the naturally predefined and artificially created water flows.

The natural water flows relevant to the modelling process include:

- Precipitation and the creation of karst runoff,
- Surface water flow,
- Flow through the porous medium,
- Transformation in karst plains,
- Evaporation from the water surface.

Artificial water flows, generated by existing or intended projects covered by the modelling process, include:

- The routing by reservoirs,
- The dam overflow,
- The flow through dam bottom outlets,
- The seepage through the dam,
- The flow through water tunnels,
- The flow through open canals,
- The flow and generation of power in hydroelectric power plants,
- The flow and power consumption in pumping stations,
- The water abstraction by users (water supply, irrigation, thermoelectric power plants).

The system was essentially decomposed into two types of entities, i.e. nodes and links, and modelling implies the generation of functional schematics which govern the simulation based on predefined rules of water distribution between the various entities.

Nodes

Nodes are model components to which the continuity equation applies.
Nodes are meeting points of one or more incoming or outgoing links.
The system was decomposed into the various entities by distinguishing fourteen types of nodes:

- Karst drainage area (entry of water into the system, transformation of rainfall into karst runoff);
- Karst plain (transformation in the karst plain);
- Reservoir (routing in the reservoir);
- Overflow (modelling of the flow over dam spillways);
- Bottom outlet (modelling of the flow through dam bottom outlets);
- Junction (node at which several incoming and outgoing links are balanced without changing the volume);
- Hydroelectric power plant (modelling of the flow through a hydroelectric power plant with power generation, includes power generation demand)
- Discharge gully (special type of junction, also includes biological minimum);
- Irrigation (managed system outflow, includes water demand for irrigation);
- Water supply (managed system outflow, includes water supply demand);
- Thermoelectric power plant (managed system outflow, includes water demand for the thermoelectric power plant);
- Pumping station (modelling of the flow through a pumping station with power consumption, includes water demand);
- Evaporation (unmanaged system outflow by evaporation from the water surface);
- Outflow (unmanaged system outflow through the ground).

A particular group of nodes is comprised of those nodes from which water invariably leaves the system (nodes of the outflow and evaporation types), while other nodes may be sub-divided into those which have a water demand (hydroelectric power plant, drainage gully, irrigation, water supply, thermoelectric power plant, pumping stations) and those which meet and/or transmit the demand.
There are specific parameters that describe the behavior of each node type.

Links

Links are model components to which the flow equation applies and transforms the inflow hydrograph of the link into the outflow hydrograph of the link. Links are also used to transmit user demand.
A link connects two nodes (inflow and outflow). The water flows from the inflow node to the outflow node. A demand is transmitted in the opposite direction.
The system breakdown into entities distinguishes between the following ten types of links:

- Karst inflow (transformation of rainfall into karst runoff);
- Surface water flow (rivers and canals);
- Groundwater flow (flow through the karst medium);
- Tunnel (flow through a tunnel);
- Direct link (flow without transformation);
- Seepage (modelling of the flow through the dam, reservoir losses);

- Evaporation (direct link to the evaporation node);
- Abstraction for irrigation (direct link to the irrigation node);
- Abstraction for water supply (direct link to the water supply node);
- Abstraction for the thermoelectric power plant (direct link to the thermoelectric power plant node).

There are specific parameters that describe the behaviour of each link type, with the exception of those, which are by nature direct.

5.1.2. Schematic representation of the system

A combination of the above mentioned nodes and links provides a model of the Trebišnjica Hydro System for various degrees of its completeness and different assumptions relating to works performance (both existing and future projects). Figure 51 is a schematic representation of the areal breakdown, which directly affects the creation of the flow in the Bregava drainage area to the Do station profile. The entities, nodes and links are identified by different symbols and designations.

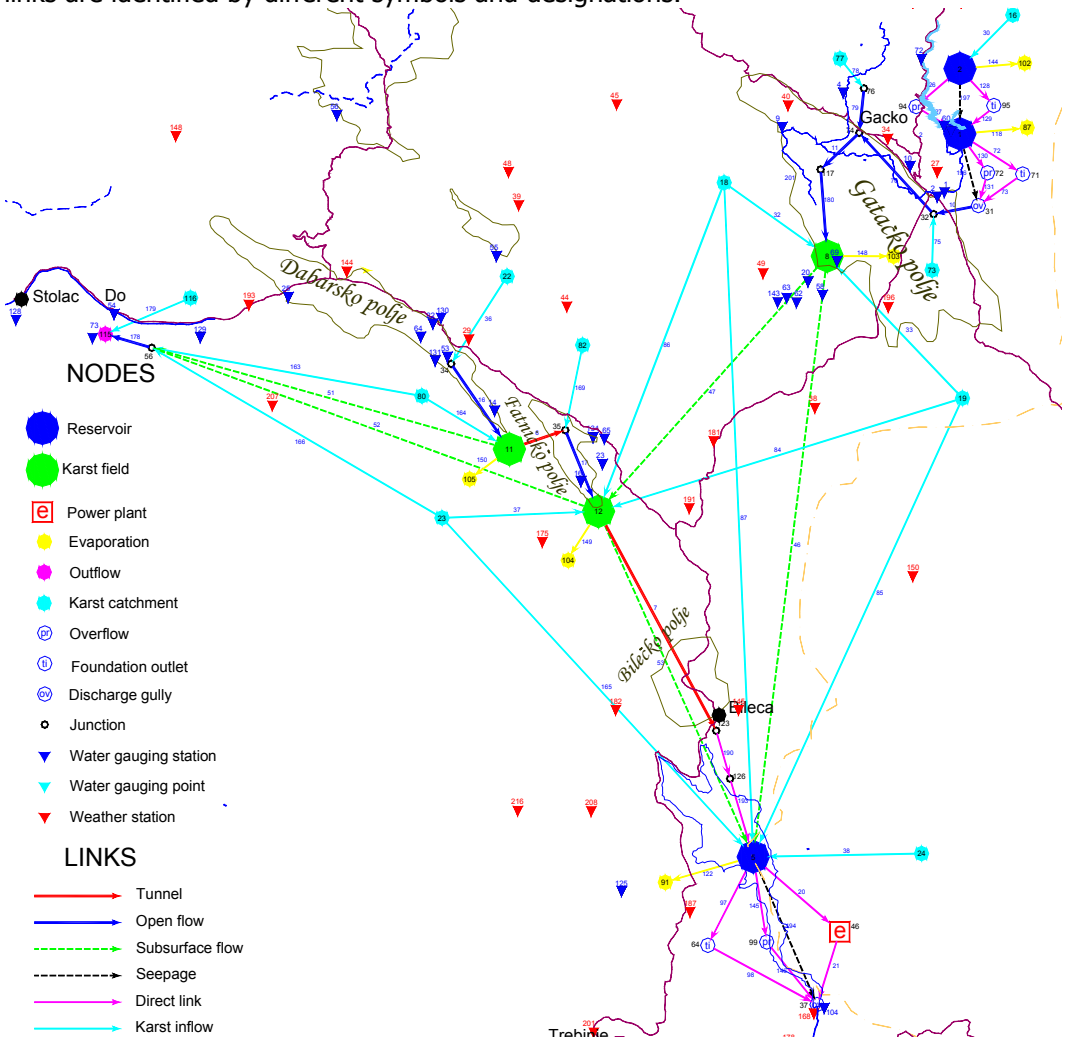

Figure 51. Decomposition of the area.

5.1.3. Mathematical (simulation) model components

The following text is a theoretical overview of the simulation model components, given separately for each entity, which are relevant to the assessment of the flow regime of the Bregava River at the Do station profile. The overview reflects both natural flow conditions and conditions created by the tunnels from Dabarsko Polje to Fatničko Polje and from Fatničko Polje to the Bileća reservoir.

Inflow generation

In karst areas water generally does not remain on the surface, but sinks into the ground where it flows in different directions and re-emerges on the terrain surface or flows directly into the sea, far from where it originally entered the ground from the surface. This means that the water, which reaches the surface from the ground, does not solely originate from rainfall or snowfall in the immediate vicinity, but is also a result of precipitation at a greater distance. Furthermore, an area experiencing heavy precipitation may be very poor in surface water, due to immediate sinking into the ground from where ongoing flow occurs.

The phenomena governing water and water flow generation in a karst area cannot be described by conventional equations addressing the transformation of rainfall into runoff. The development of the Trebišnjica Hydro System simulation model thus included the development of a mathematical model to address in parallel the rainfall-to-runoff transformation and the water flow through a karst medium. For the same reason inflows which characterize a drainage area are not determined, as would be the standard practice, but the summary flow that reaches all nodes to which it flows through the ground is determined to represent the capacity of the drainage area.

As indicated in the preceding sections, a drainage area is represented by the karst drainage area node, and the flow from the drainage area to the node is represented by the karst inflow link. The model which describes the process of precipitation-to-runoff transformation and the flow through a karst medium, developed in parallel with the preparation of the present document, does not specifically address the karst drainage area and karst inflow entities. Instead, they are treated as a single entity.

There are several weather stations in each drainage area, but data are available from only some of these station and they are considered to be representative. The drainage area precipitation is determined on the basis of precipitation at representative weather stations.

Karst drainage area A including MS weather stations with available data ($m = 1,2,...,MS$) is considered. The water reaching the karst drainage area in the form of rainfall or snowfall immediately sinks into the ground and flows in different directions, towards nodes B_i. The number of nodes which the water enters is n_B ($i = 1,2,...,n\_B$).

The basic assumption is that the water, which at some point falls onto karst drainage area A and immediately flows into the ground, re-emerges on the surface at nodes B_i at different times. Therefore, karst inflow modeling does not include the determination of the drainage area runoff at a particular time (entry into the karst inflow link), but instead the determination of the amount of water from karst drainage area A which flows to and reaches node B_i (outflow from the karst inflow link) at time k.

At any time $j\,(j = 1,2,...,k)$, typical rainfall which flows from karst drainage area A to node B_i is determined from the equation:

$$P_A^{B_i}(j) = kp_A^{1B_i} \cdot P_A^1(j) + kp_A^{2B_i} \cdot P_A^2(j) + ... + kp_A^{MS_A B_i} \cdot P_A^{MS_A}(j) = \sum_{m=1}^{MS_A} kp_A^{m\,B_i} \cdot P_A^m(j)$$

where

$kp_A^{m\,B_i}$ is a pondered value that defines which portion of the precipitation reaching weather station m gravitates to node B_i at time j.

The condition $\sum_{i=1}^{n\_B} kp_A^{mB_i} = 1$ must be satisfied for each of the MS weather stations.

The amount of water from karst drainage area A which flows through the ground and reaches node B_i (outflow from karst inflow link) is determined from the equation

$$QI_{ABi}(k) = PS^1_{ABi} \cdot \sum_{j=1}^{k} P_A^{B_i}(j) \cdot TFp(k-j+1)$$

where

TFp is the rainfall transformation function obtained from the equation

$$TFp(i) = \frac{\Delta t}{PS^3_{AB_i} \cdot (PS^2_{AB_i} - 1)!} \cdot \left(\frac{i}{PS^3_{ABi}}\right)^{PS^2_{ABi}-1} \cdot e^{-\frac{i}{PS^3_{AB_i}}},$$

$PS^1_{AB_i}$ is a parameter with the dimension $\left[\frac{m^2}{s}\right]$,

$PS^2_{AB_i}$ is a dimensionless parameter, and

$PS^3_{AB_i}$ is a parameter with a time dimension [day].

The TFp(i) transformation function shape depends on the parameters PS^3_{AB} and PS^2_{AB} which are subject to calibration based on the (known) precipitation in the watershed and the discharge profile at the watershed outlet.

The obtained outflows from the karst inflow links can then be used to determine the total capacity of karst drainage area A at time k, bearing in mind that it does not reflect a single locality.

$$Q_A(k) = QI_{AB_1}(k) + QI_{AB_2}(k) + \ldots QI_{AB_i}(k) + QI_{ABn\_B}(k) = \sum_{i=1}^{n\_B} QI_{AB_i}(k)$$

Entered total daily precipitation data series are input data for the generation of the inflow data series.
The outputs resulting from the entry of inflow data series are the data series of daily flows at the outlets of the links, which originate from the specific karst drainage area used to determine the inflow.

Karst plain and reservoir

A karst plain is an area, which retains water intermittently. Water may reach the plain either from surface flow or from the subsurface of the drainage area or from another plain. Plain drainage may be unmanaged: through the ground, through surface flow or by evaporation, and managed: by means of waterworks (belonging to different users).
A reservoir is a limited storage volume in which the water level is maintained within a predefined range, generally at the normal backwater elevation. It is fed by surface water, groundwater and the delivery of water via waterworks (tunnels). Water from the

reservoir may be released via the power plant, the spillway and the bottom outlet, as well as by seepage and evaporation from the water surface.
A karst plain is described by a volume curve and a surface curve. A reservoir, in addition to these indicators, requires the normal backwater elevation.
The figure below shows the reservoir or plain summary inflow hydrograph and reservoir or plain summary outflow hydrograph.

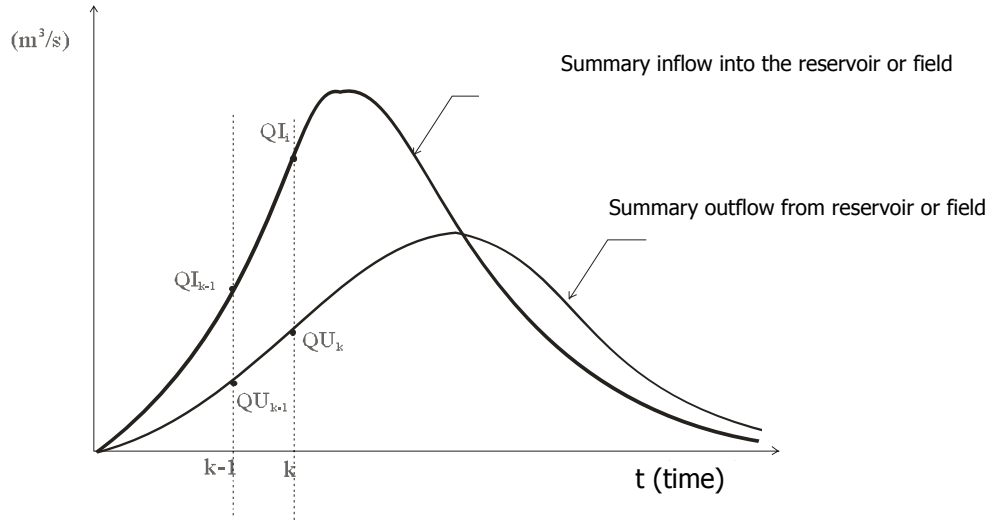

The status of the reservoir or plain at time k is described by the equation:

$$\frac{\sum_{m=1}^{M} QIZ_m^k + \sum_{m=1}^{M} QIZ_m^{k-1}}{2} - \frac{\sum_{n=1}^{N} QUL_n^k + \sum_{n=1}^{N} QUL_n^{k-1}}{2} - \frac{VIS^k}{\Delta t} - \sum_{i=1}^{I} QR_i^k = \frac{V^k - V^{k-1}}{\Delta t}$$

where

M is the number of links which enter the reservoir or karst plain,

QIZ_m^k are the outflows from the m[th] link ($m = 1,2,...,M$) which enters the reservoir at time k,

N is the number of links which leave the plain. In the case of a reservoir, $N = 1$ and is related to overflow,

QUL_n^k are inflows to the n[th] link ($n = 1,2,...,N$) which leaves the reservoir or plain at time k,

VIS^k is the evaporation from the water surface during the period Δt between time $k-1$ and time k,

I is the number of reservoir or plain water users, and

QR_i^k is the average flow to the i[th] user ($i = 1,2,...,I$) for the period Δt.

V^k is the water capacity in the field or reservoir in the time interval k

When the known terms for time k are moved to the left side of the said equation, it becomes:

$$\frac{\sum_{m=1}^{M} QIZ_m^k + \sum_{m=1}^{M} QIZ_m^{k-1}}{2} - \frac{\sum_{n=1}^{N} QUL_n^{k-1}}{2} - \frac{VIS^k}{\Delta t} - \sum_{i=1}^{I} QR_i^k = \frac{V^k}{\Delta t} + \frac{\sum_{n=1}^{N} QUL_n^k}{2}$$

Based on the reservoir or plain volume curve and the outflow curves, an accompanying function is created on the right side of the equation and, for the known left side of the equation at time k using the accompanying function, the outflow at time k is determined.

The said indicators which describe the reservoir or karst plain and the link outflows which enter the reservoir or karst plain are in effect the input data for the assessment of reservoir or plain status. The water level of the reservoir or plain at the initial point in time is also an input.
The outputs of reservoir/plain propagation assessment are:

- The reservoir stage hydrograph;
- The reservoir water volume; and
- The outflow hydrograph that is the sum of all inflows to the links which leave the plain or reservoir.

Overflow

Flood waves can be evacuated by overflow, which is represented in the model by the node of the same name. Overflow serves to remove high flows of predefined probability and to manage the water level and discharge in order to maintain the desired river flow conditions.

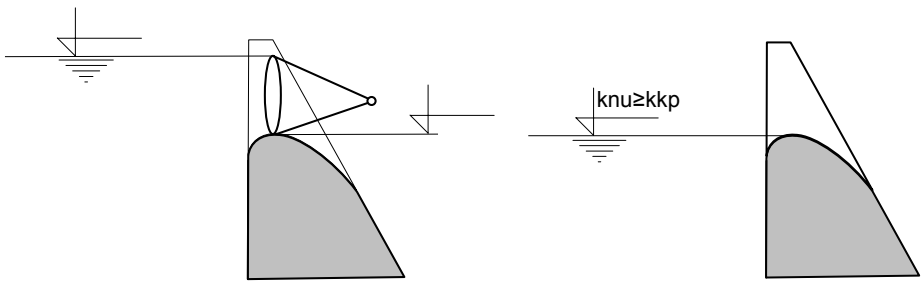

Generally speaking, the overflow capacity depends on the geometry, the hydraulic characteristics and the height of the overflow, and it amounts to

$$Q = c_q \cdot b \sqrt{2 \cdot g \cdot h_p^{\,3}}$$

where

c_q	is the overflow coefficient;
b	is the width of the overflow plain; and
h_p	is the height of the overflow stream.

The value c_q is determined by model tests or by *in situ* measurement.

The overflow curve

$$Q^k = f(H^k)$$

is generated on the basis of adopted values of the said parameters under specific conditions.
In order to determine the amount of the overflowing water, one applies the following equation which describes the reservoir volume at time k

$$\left(\frac{I^k + I^{k-1}}{2}\right) - \left(\frac{O^k + O^{k-1}}{2}\right) - OR^k = \frac{V^k - V^{k-1}}{\Delta t}$$

The auxiliary curve:

$$\frac{V^k}{\Delta t} + \frac{O^k}{2}$$

is constructed for the known reservoir volume curve and overflow curve, obtained as described above, and the maximum available overflow is determined for time k based on known input values for the previous time and current time (k and $k-1$), the overflow value for the previous time ($k-1$), the amount of water which evaporated during the period Δt and the average flow for the i^{th} user ($i = 1,2,...,I$), during the period Δt.

The actual overflow is obtained based on the requirement to maintain the normal backwater elevation in the reservoir. If it cannot be achieved, the highest possible amount of water is released via the spillway, whereby the reservoir water level is raised above the normal backwater elevation.

Input parameters for overflow assessment include:

- The overflow curve;
- The inflow hydrographs which reflect summary outflows from the links that enter the reservoir;
- The reservoir water level at the initial time; and
- The elevation of the spillway.

The outcomes of the overflow assessment are:

- The overflow hydrograph, and
- The total volume of the overflowing water.

Bottom outlet

The bottom outlet allows reservoir discharge and release of water to downstream users. In the model the bottom outlet is simulated by the node of the same name. In general terms, the reservoir may also be discharged by other means, and thus a dam need not have a bottom outlet.

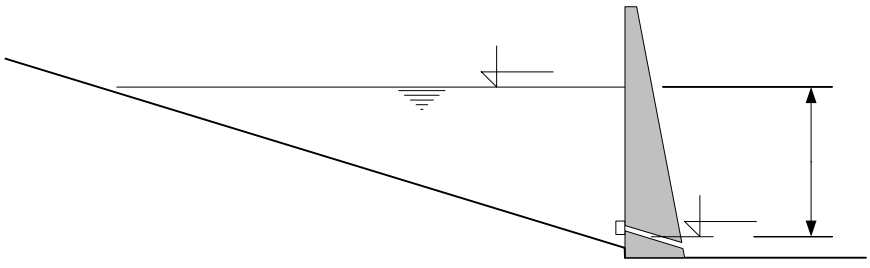

Based on the capacity of the bottom outlet for a defined constant tail water level, the following curve is constructed which describes the conveyance capacity of the outlet as a function of the water level of the reservoir:

$$Q^k = f(H^k)$$

The input parameters for the bottom outlet node are:

- The outlet conveyance capacity curve;
- The reservoir stage hydrograph; and
- The bottom outlet elevation.

The outcomes of the bottom outlet flow assessment include:

- The hydrograph, and
- The total volume of water released during the simulated period.

Junction

A junction is a node on the surface flow, which can also be its beginning or end. Junction inputs and outputs can be surface flow, karst inflow from the ground or a combination. Users can also be junction outputs. The status of a junction at time k is described by the equation

$$\sum_{m=1}^{M} QIZ_m^k = \sum_{n=1}^{N} QUL_m^k$$

where

M is the number of links which enter the node;

QIZ_m^k are outflows from the m[th] link ($m = 1,2,...,M$) which enters the node at time k;

N is the number of links which leave the node; and

QUL_n^k are inflows to the n[th] link ($n = 1,2,...,N$) which leaves the node at time k.

Input data for the junction are:

- Outflows from the links which enter the junction.

The assessment results for a junction-type node are given in the form of a hydrograph which represents the sum of the outflows from all of the links which enter the junction.

Discharge gully

The river flow downstream of the dam receives water which passed through the power plant, over the spillway, through the bottom outlet, or seeped into the river through the dam body or sides. The amount of water which reaches the watercourse in any of the above ways is summed up in the discharge gully type of node. This node is also used to define the biological minimum and/or the downstream user demand which is transmitted to the upstream entities.

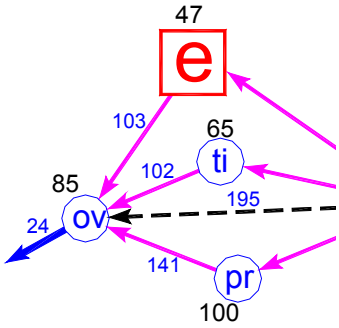

The equation which defines the status of the drainage gully at time k is:

$$Q^k = \sum_{i=1}^{N} QI_i^k$$

where

Q^k is the inflow to the discharge gully at time k;

QI_i^k is the outflow from the i^{th} link at time k; and

N is the number of links which enter the discharge gully.

The outcome of the assessment is a hydrograph that represents the sum of the outflows from the links which enter the drainage gully and which meets the demand, determined from the equation

$$\Omega^k = \frac{\sum_{i=1}^{Nk} I_i \cdot \Delta t}{\sum_{i=1}^{Nk} P_i \cdot \Delta t}$$

where

Ω^k is the indicator of meeting of quantity demand from the beginning of simulation to time k;

I_i is the delivery of water at the i^{th} time interval Δt (between time $k-1$ and time k);

P_i is the user demand at the i^{th} time interval Δt (between time $k-1$ and time k); and

N_k is the number of discrete time steps from the beginning of the simulation to time k.

Surface water flow

A stretch of the watercourse between two nodes, or two profiles – inflow and outflow, is considered. The surface water flow is assessed by applying the Muskingum method.

The Muskingum method introduces the concept of the "volume" flow (at the outlet), which is a function of the inflow and outflow at the same time instant

$$QT^k = R^2 \cdot QU^k + \left(1 - R^2\right) \cdot QI^k$$

where:

QT is the water capacity on the considered river sector (between the inlet and outlet river profile) at time k

R^1 is a method parameter representing linear dependence decrease
R^2 is a dimensionless method parameter (constant)
QI is the outlet profile discharge

The basic assumption of the Muskingum method is that the relationship between the "volume" flow QT^k, in time step Δt, and the water volume along the stretch between the inflow and outflow is linear, i.e. that the following relation applies:

$$V^k = R^1 \cdot QT^k = R^1 \cdot \left(R^2 \cdot QU^k + \left(1 - R^2\right) \cdot QI^k\right)$$

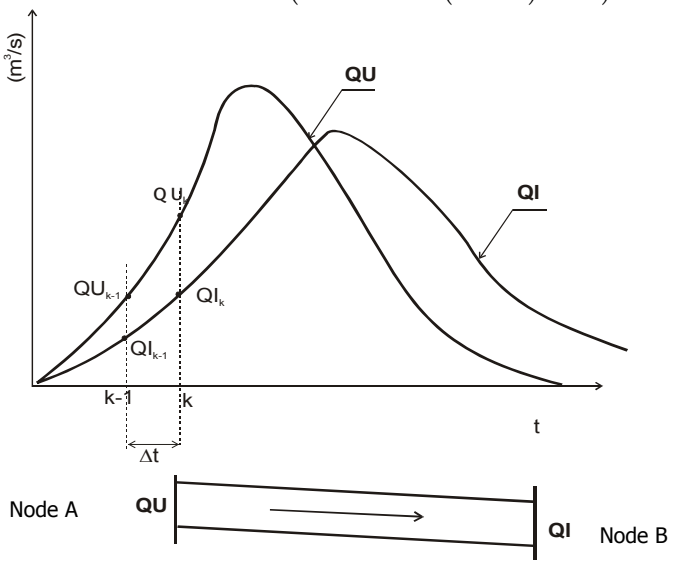

For the period of discretisation Δt the volume change between the inflow and outflow profiles amounts to

$$\Delta V = V^k - V^{k-1} = R^1 \cdot \left(R^2 \cdot QU^k + \left(1 - R^2\right) \cdot QI^k\right) - R^1 \cdot \left(R^2 \cdot QU^{k-1} + \left(1 - R^2\right) \cdot QI^{k-1}\right)$$

If the continuity equation is written for the inflow and outflow profiles and the discretisation period Δt, then

$$\Delta V = \frac{\left(QU^{k-1} + QU^k\right)}{2} - \frac{\left(QI^{k-1} + QI^k\right)}{2}$$

By equating ΔV from the continuity equation and the volume change equation as a function of "volume" flow, and after arrangement

$$QI^k = C_0 \cdot QU^k + C_1 \cdot QU^{k-1} + C_2 \cdot QI^{k-1}$$

or, if one takes into account that each link is defined by its own number, then

$$QI^k_{\text{link num.}} = C_0 \cdot QU^k_{\text{link num.}} + C_1 \cdot QU^{k-1}_{\text{link num.}} + C_2 \cdot QI^{k-1}_{\text{link num.}}$$

applies to the specific surface flow type of link, whereby

$$C_0 = \frac{0.5 \cdot \Delta t - R^1_{\text{link num.}} \cdot R^2_{\text{link num.}}}{R^1_{\text{link num.}} \cdot \left(1 - R^2_{\text{link num.}}\right) + 0.5 \cdot \Delta t}$$

$$C_1 = \frac{0.5 \cdot \Delta t + R^1_{\text{link num.}} \cdot R^2_{\text{link num.}}}{R^1_{\text{link num...}} \cdot \left(1 - R^2_{\text{link num.}}\right) + 0.5 \cdot \Delta t}$$

$$C_2 = \frac{R^1_{\text{link num.}} \cdot \left(1 - R^2_{\text{link num.}}\right) - 0.5 \cdot \Delta t}{R^1_{\text{link num.}} \cdot \left(1 - R^2_{\text{link num.}}\right) + 0.5 \cdot \Delta t}$$

The condition that needs to be satisfied is $C_0 + C_1 + C_2 = 1$.

The coefficients $C_0,\ C_1\ and\ C_2$ are determined on the basis of parameters which characterize the surface flow link

$R^1_{\text{link num.}}$ and $R^2_{\text{link num.}}$, where

$R^2_{\text{link num.}}$ is the dimensionless parameter $0 \le R^2_{\text{link num.}} \le 0.5$, and

$R^1_{\text{link num.}}$ is a parameter with a time dimension, which satisfies the condition

$$R^1_{\text{link num.}} \le \frac{\Delta t}{2 \cdot R^2_{\text{link num.}}}$$

Input data for surface flow assessment include:

- The link inflow hydrograph, and
- The parameters $R^1_{\text{link num.}}$ and $R^2_{\text{link num.}}$.

The output is

- The link outflow hydrograph.

Flow through a karst medium (water retained in the plain)

When flow through a karst medium was modeled it was assumed that the amount of water which reaches the downstream node B from node A is a function of the inflow. Node A may be a plain or junction. If it is a plain, the amount of sinking water depends on the water level in the plain and the outflow capacity. In the case of a junction it is determined as a function of inflow to the junction.

In view of the fact that the flow velocity through a karst medium is much lower than in the case of surface water flow, it is clear that the outflow magnitude in the case of flow through a karst medium is influenced by outflows from several previous time steps, and not solely from the previous time step as in the case of surface flow.

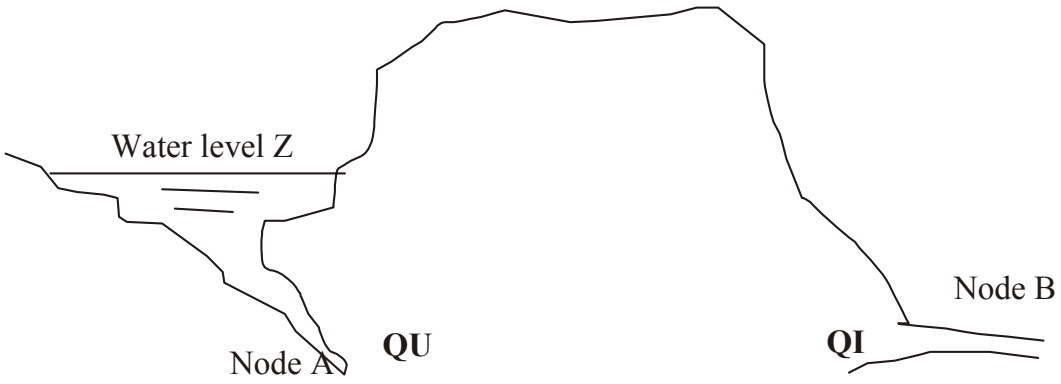

Water flow through a karst medium is described by the equation

$$\mathrm{QI}^{\mathrm{k}}_{\text{link num.}} = \mathrm{PT}^{1}_{\text{link num.}} \cdot \sum_{\mathrm{j}=1}^{\mathrm{k}} \mathrm{QU}^{\mathrm{j}}_{\text{link num.B}} \cdot \mathrm{TFq}(\mathrm{k}-\mathrm{j}+1)$$

Water from node A sinks into the ground and, following subsurface paths, reaches one or more nodes (maximum l) where it re-emerges on the surface. The parameters $PT^{1}_{\text{link num.}}$ define which portion of water from node A flows along subsurface paths to one of the outflow nodes. The condition to be satisfied is

$$\sum_{l} \mathrm{PT}^{1}_{\text{link num.}} \leq 1 .$$

At time k the flow which has reached node B is the sum of transformed flows that reach the subsurface (node A) at times $\mathrm{k}-1, \mathrm{k}-2, \ldots, \mathrm{k}-\mathrm{n}+1$.

The flow transformation function is defined for the link parameters $PT^{2}_{\text{link num.}}$ and $PT^{3}_{\text{link num.}}$ by the equations

$$\mathrm{TFq}(\mathrm{i}) = \frac{\Delta \mathrm{t}}{\mathrm{PT}^{3}_{\text{link num.}} \cdot \Delta \mathrm{t} \cdot \left(\mathrm{PT}^{2}_{\text{link num.}} - 1\right)!} \cdot \left(\frac{\mathrm{i} \cdot \Delta \mathrm{t}}{PT^{3}_{\text{link num.}} \cdot \Delta \mathrm{t}} \right)^{\mathrm{PT}^{2}_{\text{link num.}} - 1} \cdot \mathrm{e}^{-\frac{\mathrm{i} \cdot \Delta \mathrm{t}}{\mathrm{PT}^{3}_{\text{link num.}} \cdot \Delta \mathrm{t}}}$$

$$\mathrm{TFq}(\mathrm{i}) = \frac{1}{\mathrm{PT}^{3}_{\text{link num.}} \cdot \left(\mathrm{PT}^{2}_{\text{link num.}} - 1\right)!} \cdot \left(\frac{\mathrm{i}}{PT^{3}_{\text{link num.}}} \right)^{\mathrm{PT}^{2}_{\text{link num.}} - 1} \cdot \mathrm{e}^{-\frac{\mathrm{i}}{PT^{3}_{linknum.}}}$$

The parameter $PT^{3}_{\text{link num.}}$ has a time dimension, while the parameter $PT^{2}_{\text{link num.}}$ is dimensionless.
The input data for the assessment of the flow through a karst medium include:

- The link inflow hydrograph, and
- The parameters $PT^{1}_{\text{link num.}}$, $PT^{2}_{\text{link num}}$ and $PT^{3}_{\text{link num.}}$.

The output is the link output hydrograph.

Flow through a karst medium (no water in the plain)

From the karst plain outflow generation process it is evident that outflow occurs even though no water has accumulated in the plain. This is a consequence of exhausting underground spaces where water is temporarily retained after a rainfall event, depending on the nature of the cavities and pores and the geometry. In order to model this occurrence, it is assumed that beneath the plain level there is a certain volume filled with water, which is gradually discharged via a karst spring located at a lower elevation, whose yield is Q. During a relatively long dry period, the water volume V in the said underground spaces is gradually discharged, and the capacity of the spring on account of the water from the said volume is Q_1. Such yield is directly related to the water level status in the imaginary subsurface volume h_1, or the water volume status, which is also a function of h_1.

In the river discharge (flow) generation modelling process for the karst medium it is assumed that there is a direct relationship between the water volume in the said subsurface spaces and the water level h1, i.e. there is an unknown volume curve (see figure) $\mathrm{V} = \mathrm{f}(\mathrm{h}_1)$, being a parameter that is calibrated. The subsurface outflow during

the dry period is approximated by the outflow from a fully charged water tank, where water inflow to the tank is equal to zero.

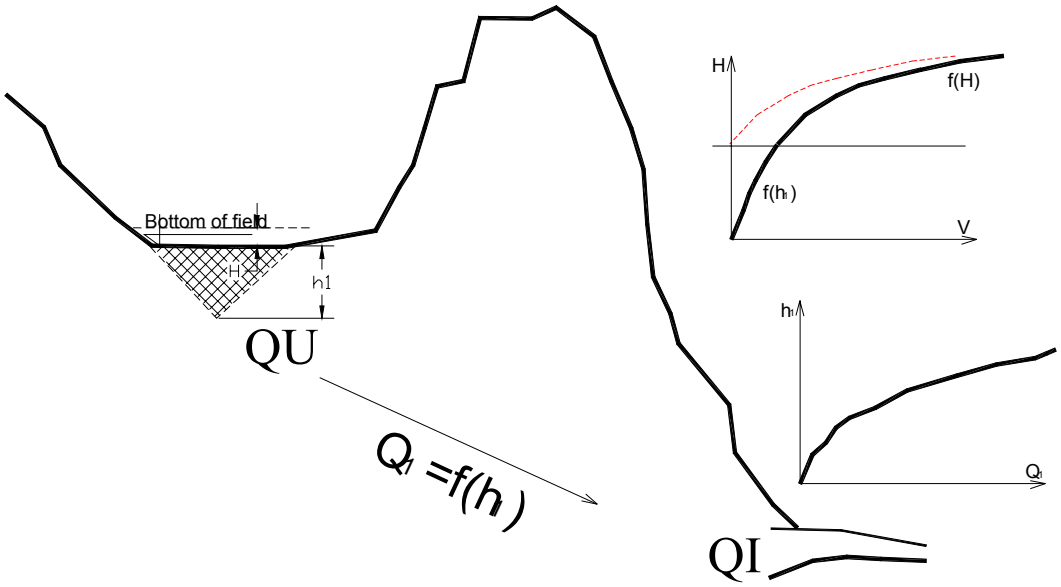

Flow through a tunnel

Flow through a tunnel is modeled by means of the tunnel-type link. The flow through a tunnel may or may not be pressurized. Pipe outflow may be free or submerged. The losses which occur in the course of the flow through a tunnel include local losses (valves, elbows, varying geometry, etc.) and line losses (friction). The losses and boundary conditions are determined in order to construct the outflow curve $Q(Z)$.

The tunnel is a link between the reservoir or karst plain (nodes characterized by the water level) and the power plant or junction.
The input parameters for tunnel flow assessment include:

- The outflow curve, and
- The reservoir or plain stage hydrograph.

The output is the outflow hydrograph.

Direct link

A direct link is a link designed to transmit both the demand to upstream entities and the outcome of a status change to downstream users. The status of the i^{th} link at time k is described by the equation

$$QI_i^k = QU_i^k$$

where

QU_i^k is the inflow to the i^{th} link at time k, and

QI_i^k is the outflow from the i^{th} link at time k.

The output is the outflow hydrograph.

Seepage

Seepage under the dam body and sides is particularly pronounced in karst areas such as that of the Trebišnjica Hydro System. The model simulates this process by a seepage-type link. The link represents a combination of the seepage node and a direct link, but considering necessity of occurrence it has been replaced by a single entity. The input parameters are the seepage curve, which in the general case may be determined by measurement but is in practice obtained from the balance equation, and the reservoir stage hydrograph.
The output is the seepage hydrograph.

Evaporation from the water surface

Evaporation from the water surface is a permanent process which depends on the water and air temperatures, the air humidity deficit, the wind speed, the vapor pressure and other weather factors, and is a very important component of the water balance. It is measured by means of evaporation pan – evaporimeters, which come in different shapes. Class A pans are the most commonly used in the hydro-meteorological practice of this part of the world. The evaporation from larger and deeper water surfaces, such as a river reservoir, differs from evaporation from a pan due to differences in the water temperature increase between a pan and the water surface of a lake. In the hydrological practice it is common to apply a reduction coefficient of the order of 0,7 for the difference between evaporation from a pan and evaporation from deeper water surfaces.
Pan evaporation is generally measured during the warm part of the year and thus evaporation data are not available for the entire calendar year. Furthermore, even during that part of the year most weather stations do not measure evaporation continuously. Since evaporation data are required for a longer continuous period, especially if one takes into account the reservoir water balance where evaporation from the water surface is a water "loss" from the viewpoint of hydroelectric power generation, it is necessary to establish an empirical relationships between evaporation and other weather parameters which directly influence the evaporation process, i.e. those that are recorded in the considered area. Such relationships are applied when assessing evaporation for periods during which it was not measured.
In the specific case, i.e. that of assessing the total daily evaporation from the water surface of the Bileća reservoir and the karst plains in the drainage area of the Bregava, the following nonlinear function applies:

$$E^k = C_m^j \left(a \cdot T^{k\,3} + b \cdot T^{k\,2} + cT^k + d \right)$$

where

E^k is the total daily evaporation from the water surface at time k;
C_m^j is the monthly coefficient of evaporation; and
a, b, c and d are parameters (regression coefficients).

Model inputs are average daily air temperatures and model parameters include monthly evaporation coefficients (see following table) and regression coefficients. The outputs are the total daily evaporation expressed in millimeters and the total daily volume of water which has evaporated.

The free surface evaporation computation for the Bileća Reservoir and the karstic fields has been performed using established regression dependence between the evaporation and the mean daily air temperature.

Since the relevant data for computing the evaporation (air deficiency and wind velocity data) were not available during the preparation of the Trebišnjica Hydro Information System Phase I, to enable an indirect assessment of these factors, regression equations were formed for each month separately, by introducing the coefficient Cm.

The regression coefficients were obtained using the available data series on evaporation of the A class evaporator in the Bileća Reservoir and the corresponding data on mean daily air temperatures. All parameters in the regression equations (a, b, c, m and n) were determined by a least square method. The monthly coefficients Cm were determined from the relation between the monthly evaporation sum and the sum of daily evaporation sums for the available data series.

Table 6. Values of monthly evaporation coefficients C_m

Jan	Feb	Mar	Apr	May	Jun	Jul	Aug	Sep	Oct	Nov	Dec
0.01	0.07	0.25	0.54	0.73	0.82	0.81	0.81	0.7	0.63	0.33	0.03

5.1.4. Use of data

Data required to apply the model in practice and to simulate the flow of the Bregava at the Do station profile were obtained from the IJC database created for the development of the Trebišnjica HIS. The database includes the following:

- Hydro-meteorological data (river stages, discharges, precipitation, air temperatures, water vapour pressure, wind speeds and evaporation);
- System configuration (reservoir surface and volume curves, overflow and intake elevations, spillway and intake structure capacities);
- General information on the entities (numeration, types, designations, descriptions, photographs and current IPS status indicators);
- Information on the hydrographic network: springs, sinks, groundwater and surface water flows, lakes and karst plains);
- Hydrogeologic data: piezometric groundwater levels;
- Information on data stations: types, identification, kinds of measurement;
- Hydrologic occurrences: categories, types, units of measure and descriptions; and
- Indicators of typical occurrences relating to hydrologic data.

The database for the considered area reflects the information provided by the meteorological team (Chapter 3). A chronological overview of the data available for the period from 1 January 1961 to 31 December 2003 is given in Figure 52 - Figure 54.

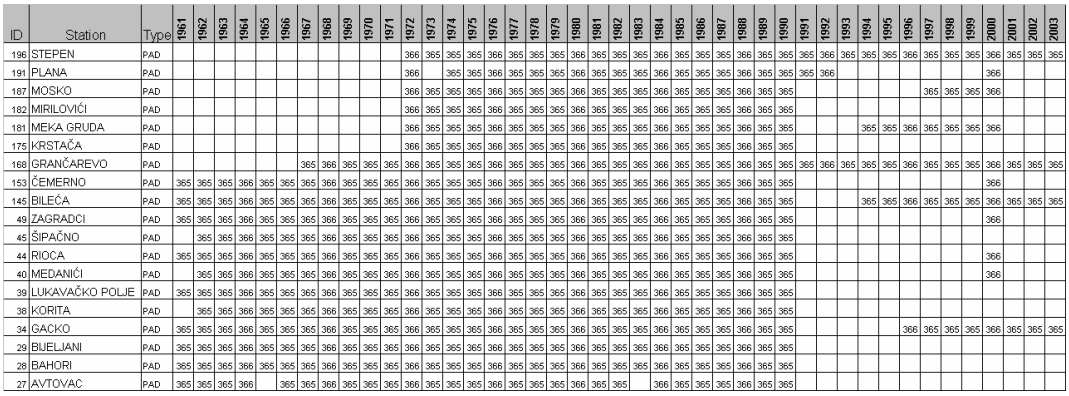

ID	Station	Type	1961	1962	1963	1964	1965	1966	1967	1968	1969	1970	1971	1972	1973	1974	1975	1976	1977	1978	1979	1980	1981	1982	1983	1984	1985	1986	1987	1988	1989	1990	1991	1992	1993	1994	1995	1996	1997	1998	1999	2000	2001	2002	2003
196	STEPEN	PAD												366	365	365	365	366	365	365	365	366	365	365	365	366	365	365	365	366	365	365	365	366	365	365	365	366	365	365	365	366	365	365	365
191	PLANA	PAD												366		365	365	366	365	365	365	366	365	365	365	366	365	365	365	366	365	365	365	366									366			
187	MOSKO	PAD												366	365	365	365	366	365	365	365	366	365	365	365	366	365	365	365	366	365	365							365	365	365	366			
182	MIRILOVIĆI	PAD												366	365	365	365	366	365	365	365	366	365	365	365	366	365	365	365	366	365	365	365												
181	MEKA GRUDA	PAD												366	365	365	365	366	365	365	365	366	365	365	365	366	365	365	365	366	365	365	365			365	365	366	365	365	365	366			
175	KRSTAČA	PAD												366	365	365	365	366	365	365	365	366	365	365	365	366	365	365	365	366	365	365	365												
168	GRANČAREVO	PAD							365	366	365	365	365	366	365	365	365	366	365	365	365	366	365	365	365	366	365	365	365	366	365	365	365	366	365	365	365	366	365	365	365	366	365	365	365
153	ČEMERNO	PAD	365	365	365	366	365	365	365	366	365	365	365	366	365	365	365	366	365	365	365	366	365	365	365	366	365	365	365	366	365	365										366			
145	BILEĆA	PAD	365	365	365	366	365	365	365	366	365	365	365	366	365	365	365	366	365	365	365	366	365	365	365	366	365	365	365	366	365	365			365	365	366	365	365	365	366	365	365	365
49	ZAGRAĐCI	PAD	365	365	365	366	365	365	365	366	365	365	365	366	365	365	365	366	365	365	365	366	365	365	365	366	365	365	365	366	365	365										366			
45	ŠIPAČNO	PAD		365	365	366	365	365	365	366	365	365	365	366	365	365	365	366	365	365	365	366	365	365	365	366	365	365	365	366	365	365													
44	RIOCA	PAD	365	365	365	366	365	365	365	366	365	365	365	366	365	365	365	366	365	365	365	366	365	365	365	366	365	365	365	366	365	365										366			
40	MEDANIĆI	PAD		365	365	366	365	365	365	366	365	365	365	366	365	365	365	366	365	365	365	366	365	365	365	366	365	365	365	366	365	365										366			
39	LUKAVAČKO POLJE	PAD	365	365	365	366	365	365	365	366	365	365	365	366	365	365	365	366	365	365	365	366	365	365	365	366	365	365	365	366	365	365													
38	KORITA	PAD		365	365	366	365	365	365	366	365	365	365	366	365	365	365	366	365	365	365	366	365	365	365	366	365	365	365	366	365	365													
34	GAĆKO	PAD	365	365	365	366	365	365	365	366	365	365	365	366	365	365	365	366	365	365	365	366	365	365	365	366	365	365	365	366	365	365					366	365	365	365	366	365	365	365
29	BIJELJANI	PAD	365	365	365	366	365	365	365	366	365	365	365	366	365	365	365	366	365	365	365	366	365	365	365	366	365	365	365	366	365	365													
28	BAHORI	PAD	365	365	365	366	365	365	365	366	365	365	365	366	365	365	365	366	365	365	365	366	365	365	365	366	365	365	365	366	365	365													
27	AVTOVAC	PAD	365	365	365	366		365	365	366	365	365	365	366	365	365	365	366	365	365	365	366	365	365		366	365	365	365	366	365	365													

Figure 52. Overview of meteorological data (precipitation)

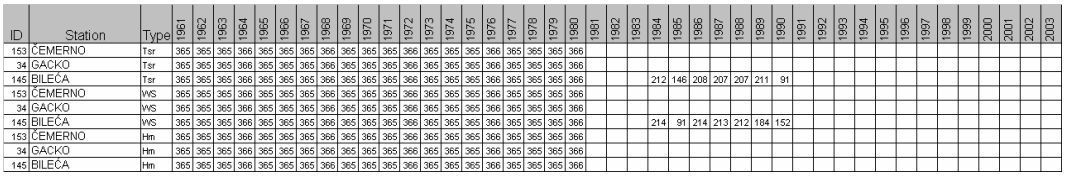

ID	Station	Type	1961	1962	1963	1964	1965	1966	1967	1968	1969	1970	1971	1972	1973	1974	1975	1976	1977	1978	1979	1980	1981	1982	1983	1984	1985	1986	1987	1988	1989	1990	1991	1992	1993	1994	1995	1996	1997	1998	1999	2000	2001	2002	2003
153	ČEMERNO	Tsr	365	365	365	366	365	365	365	366	365	365	365	366	365	365	365	366	365	365	365	366																									
34	GAĆKO	Tsr	365	365	365	366	365	365	365	366	365	365	365	366	365	365	365	366	365	365	365	366																									
145	BILEĆA	Tsr	365	365	365	366	365	365	365	366	365	365	365	366	365	365	365	366	365	365	365	366				212	146	208	207	207	211	91															
153	ČEMERNO	WS	365	365	365	366	365	365	365	366	365	365	365	366	365	365	365	366	365	365	365	366																									
34	GAĆKO	WS	365	365	365	366	365	365	365	366	365	365	365	366	365	365	365	366	365	365	365	366																									
145	BILEĆA	WS	365	365	365	366	365	365	365	366	365	365	365	366	365	365	365	366	365	365	365	366				214	91	214	213	212	184	152															
153	ČEMERNO	Hm	365	365	365	366	365	365	365	366	365	365	365	366	365	365	365	366	365	365	365	366																									
34	GAĆKO	Hm	365	365	365	366	365	365	365	366	365	365	365	366	365	365	365	366	365	365	365	366																									
145	BILEĆA	Hm	365	365	365	366	365	365	365	366	365	365	365	366	365	365	365	366	365	365	365	366																									

Figure 53. Overview of meteorological data (Temperature; Wind speed; Humidity)

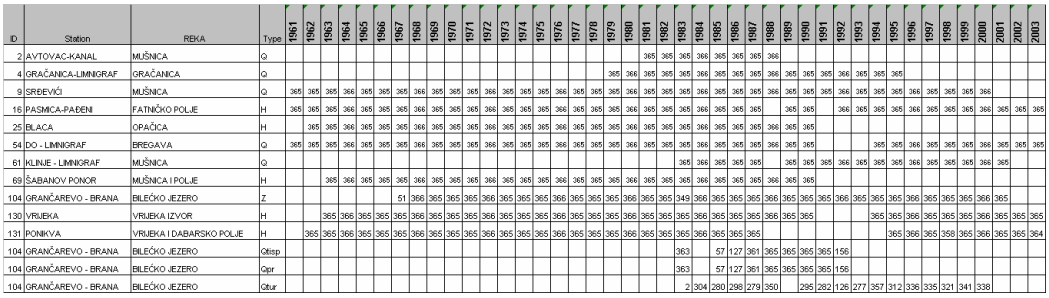

ID	Station	REKA	Type	1961	1962	1963	1964	1965	1966	1967	1968	1969	1970	1971	1972	1973	1974	1975	1976	1977	1978	1979	1980	1981	1982	1983	1984	1985	1986	1987	1988	1989	1990	1991	1992	1993	1994	1995	1996	1997	1998	1999	2000	2001	2002	2003
2	AVTOVAC-KANAL	MUŠNICA	Q																						365	365	365	366	365	365	366														
4	GRAČANICA-LIMNIGRAF	GRAČANICA	Q																					365	366	365	365	366	365	365	365	366	365	365	365	365	365	365								
9	SRĐEVIĆI	MUŠNICA	Q	365	365	365	366	365	365	365	366	365	365	365	366	365	365	365	366	365	365	365	366	365	365	365	365	366	365	365	365	366	365	365	365	366	365	365	365	365	366			
16	PASMICA-PAĐENI	FATNIČKO POLJE	H	365	365	365	366	365	365	365	366	365	365	365	366	365	365	365	366	365	365	365	366	365	365	365	365	366	365	365	365		365	365		366	365	365	365	366	365	365	366	365	365
25	BLACA	OPAČICA	H		365	365	366	365	365	365	366	365	365	365	366	365	365	365	366	365	365	365	366	365	365	365	365	366	365	365	365	366	365	365											
54	DO - LIMNIGRAF	BREGAVA	Q	365	365	365	366	365	365	365	366	365	365	365	366	365	365	365	366	365	365	365	366	365	365	365	365	366	365	365	365	366	365	365			365	365	366	365	365	365	366	365	365
61	KLINJE - LIMNIGRAF	MUŠNICA	Q																								365	366	365	365	365		365	365	365	366	365	365	365	365	365	366	365			
69	ŠABANOV PONOR	MUŠNICA I POLJE	H				365	366	365	365	366	365	365	365	366	365	365	365	366	365	365	365	366	365	365	365	365	366	365	365	365	366	365	365											
104	GRANČAREVO - BRANA	BILEĆKO JEZERO	Z						51	366	365	365	365	366	365	365	365	366	365	365	365	366	365	365	365	366	365	365	349	366	365	365	365	366	365	365	365	365	366	365	365	365	366	365	
130	VRIJEKA	VRIJEKA IZVOR	H			365	366	365	365	365	366	365	365	365	366	365	365	365	366	365	365	365	366	365	365	365	365	366	365	365	365	366	365	365	365			365	365	366	365	365	365	366	365	365
131	PONIKVA	VRIJEKA I DABARSKO POLJE	H		365	365	366	365	365	365	366	365	365	365	366	365	365	365	366	365	365	365	366	365	365	365	365	366	365	365	365	365						365	366	365	358	365	366	365	365	364
104	GRANČAREVO - BRANA	BILEĆKO JEZERO	Qtisp																								363		57	127	361	365	365	365	156											
104	GRANČAREVO - BRANA	BILEĆKO JEZERO	Qpr																								363		57	127	361	365	365	365	156											
104	GRANČAREVO - BRANA	BILEĆKO JEZERO	Qtur																								2	304	280	298	279	350		295	282	126	277	357	312	336	335	321	341	338			

Figure 54. Overview of hydrological data

Missing data, which were required to run the models, were entered by applying correlation methods to all weather stations that provide model inputs.

5.1.5. Calibration and validation

The monitoring and measurement data relating to hydro-meteorological occurrences and other information about the system configuration status during the period from 1 January 1961 to 31 October 1986 were used to calibrate model parameters. It was assumed that the tunnel between Dabarsko Polje and Fatničko Polje was not operational during this time, i.e. that there was no water inflow from Dabarsko Polje to Fatničko Polje.
Model simulation parameters were checked in the calibration process against selected key data stations of the system, including:

- System outputs: the Bregava discharges at the Do gauging station and the total Trebišnjica discharges from the Bileća reservoir (discharge from the Grnčarevo HPP, spillway, bottom outlet and seepage through the dam), and
- Headwater stages for the Bileća reservoir, as well as for the Dabarsko Polje and Fatničko Polje.

The model was designed for spatial calibration of parameters, taking into account the available hydrologic data from water gauging and other data stations in the drainage area. It should be noted that the total outflow from the Trebišnjica is known in the model parameter calibration process and it is obtained from the database.

Model parameters calibration was performed starting from the topologically most upstream profiles (including the water gauging stations on the Musnica, Gracanica, Gojkovica Stream etc), artificial reservoirs (Vrba and Klinje), natural karst fields (Gatacko, Cernicko, Dabarsko and Fatnicko) up to the outlet profiles (water gauging station on the Bregava River) and structures (Bileca Reservoir on the Trebisnjica). The adopted parameter values calibrated along the upstream reach were considered constant when determining the downstream reaches runoff. The parameter values were chosen using a least square method, for discharge and water level.

The criterion for river flow simulation quality assessment in the calibration phase, as it applies to the considered drainage area, is the achievement of minimal deviation of computed outputs from the values recorded by key data stations of the system in a least square sense. A graphic interpretation of the results of model calibration is given in the form of parallel diagrams of computed and registered values, such as:

- The Bregava River hydrograph for the Do gauging station (Figure 55);
- The Bregava River discharge duration curve for the Do gauging station (Figure 56);
- The water stage diagram of the Dabarsko Polje plain (Figure 57);
- The water stage duration curve for the Dabarsko Polje plain (Figure 58);
- The water stage diagram of the Fatničko Polje plain (Fig. 7);
- The water stage duration curve for the Fatničko Polje plain (Fig. 8);
- The headwater stage diagram of Bileća reservoir (Fig. 9);
- The headwater stage duration curve for the Bileća reservoir (Fig. 10).

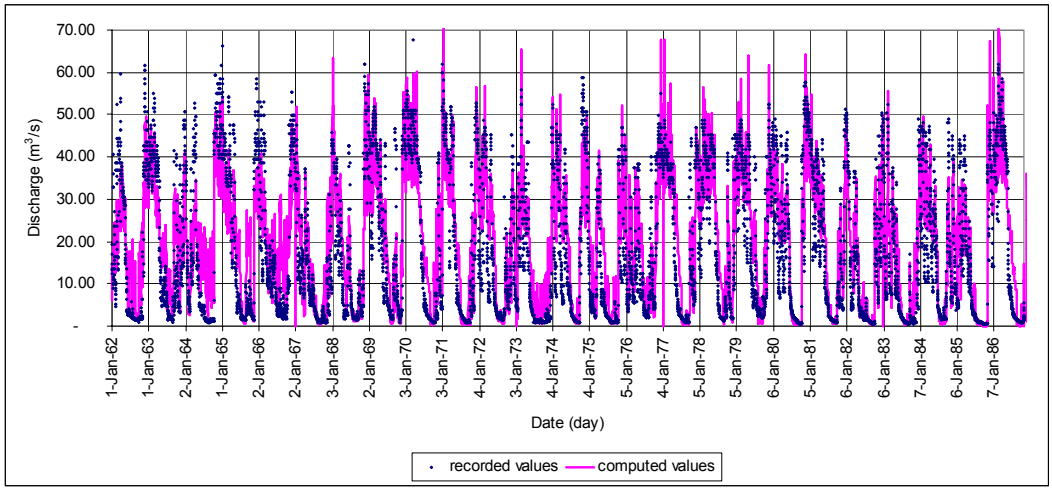

Figure 55. The Bregava River hydrograph for Do gauging station

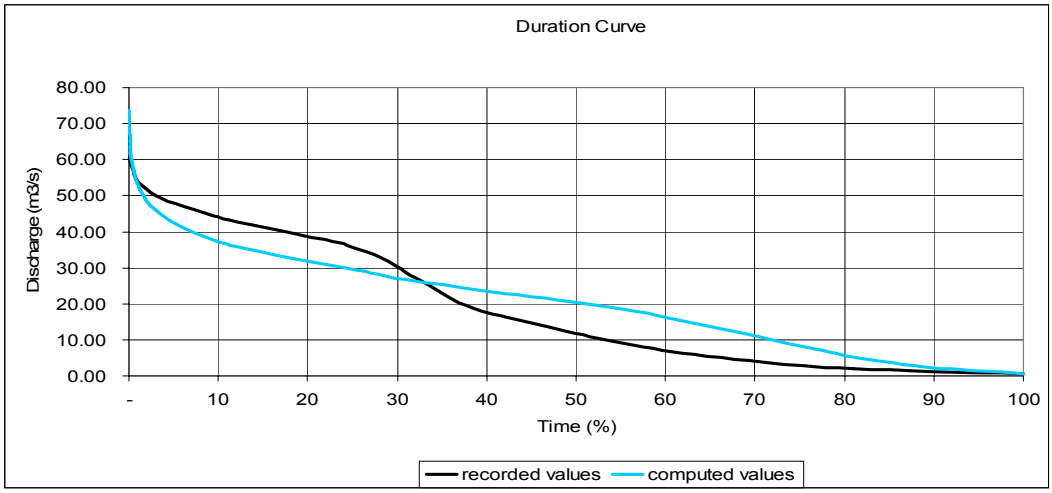

Figure 56. The Bregava River discharge duration curve for Do gauging station.

It may be concluded from the results shown above that the applied simulation model provides a good match between the computed and recorded hydrographs of the Bregava at the Do gauging station (Figure 55), both in terms of the dynamic/time of flood wave occurrence and the total amounts of water. For the considered period of model parameter identification the multi-annual average discharges are:

- Computed 19.19 m^3/s and
- Recorded 18.39 m^3/s.

The difference of 0.8 m^3/s is only 5% of the multi-annual average discharge of the Bregava at the Do gauging station profile, and this is below the accuracy tolerance for hydro-meteorological (measured and processed) data inputs.

The discharge duration curves for the Bregava River at the Do gauging station profile (Figure 56) indicate a significant difference between computed and registered discharges in the discharge duration zones of 5-30% and 35-80%. The accuracy of the basic hydro-meteorological data inputs, and particularly those for the Bregava discharges at the Do gauging station profile, is not very high. This is a consequence of very complex flow conditions in the karst medium, which cannot be adequately and accurately simulated by the applied model.

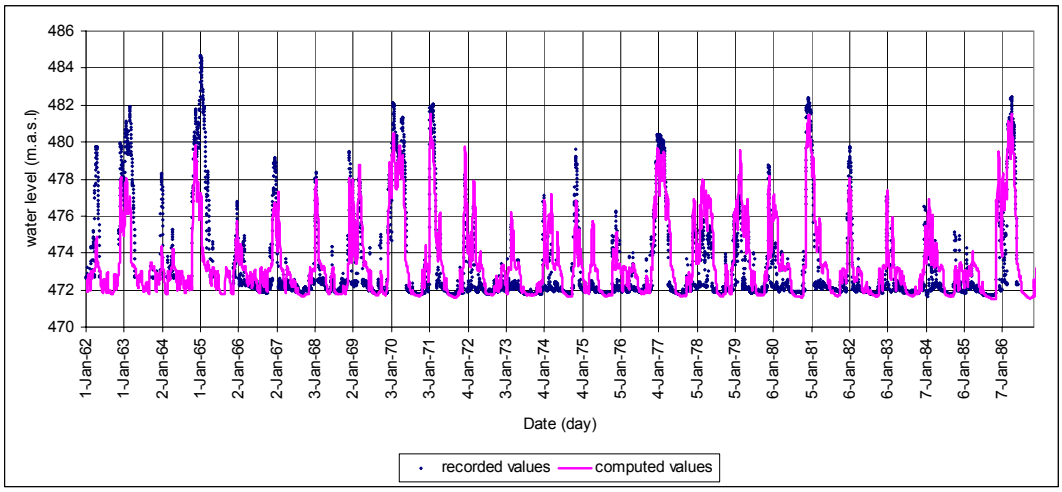

Figure 57. Water stage diagram of Dabarsko Polje

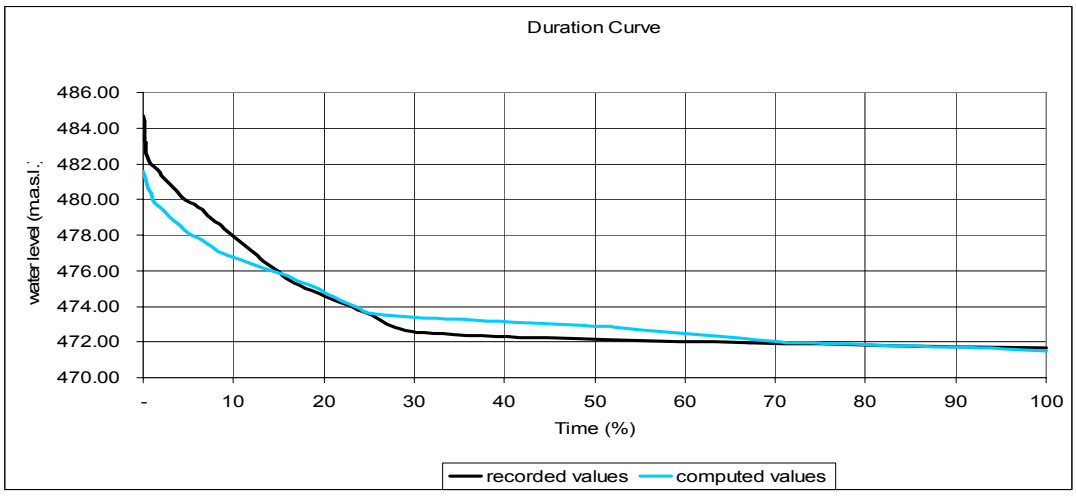

Figure 58. Water stage duration curve for Dabarsko Polje

A parallel water stage diagram of the Dabarsko Polje plain (Figure 57) indicates a very good match between computed and registered flood waves, for both extreme values/time of occurrence and multi-annual average values. The multi-annual average headwaters for the said period are:

- Computed 473.47 m asl and
- Registered 473.39 m asl

The difference of 0.08 m is negligible in view of the measurement accuracy and the relevance of a single point in space to a realistic assessment of water stages in the plain, i.e. the water volume or more accurately the dynamic volume.

Appropriate water stage duration curves for the Dabarsko Polje plain (Figure 58) indicate that a very good match is achieved between computed and registered water stages in the duration range of 10-100%. For durations under 10%, the computed values are lower than the registered values, which lead to the computed discharges of the Bregava being lower than registered during these periods (a cause-and-effect relationship).

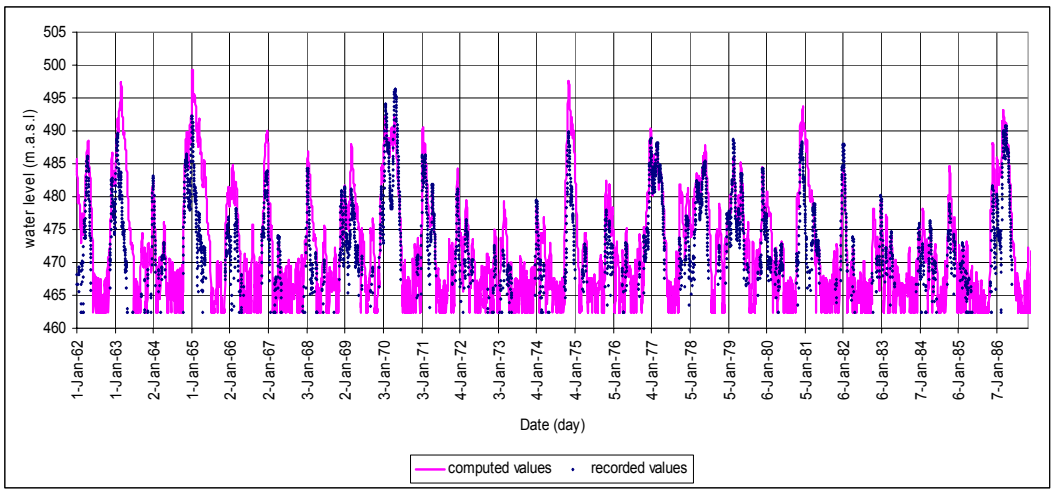

Figure 59. Water stage diagram of Fatničko Polje

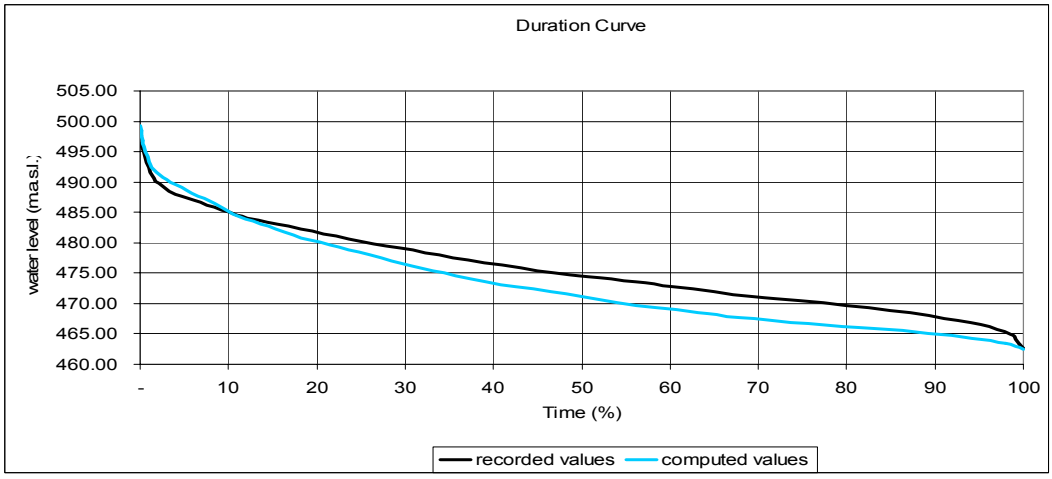

Figure 60. Water stage duration curve for Fatničko Polje

The water stage variation diagram of Fatničko Polje (Figure 59) shows that there are significant differences between computed and registered stages, and that there is an absence of water over a relatively long period. From the perspective of flood occurrence dynamics in the plain, a relatively good match was obtained between computed and registered values. The difference between computed and registered multi-annual average values is 2.73 m, and this is admissible in view of the facts mentioned above. The water stage duration curves for Fatničko Polje (Figure 60) indicate that the difference between computed and registered curves is in the duration range from 10 to 97% in the positive sense (registered stages are higher), and that the direction is reversed for short durations.